



UNIVERSITA' DI NAPOLI FEDERICO II

DOTTORATO DI RICERCA

BIOCHIMICA E BIOLOGIA CELLULARE E MOLECOLARE

XXVIII CICLO

*Novel approaches for breast cancer therapy:
exploiting fully human immunoRNases targeting
ErbB2-positive and triple-negative breast cancers*

Candidate

Chiara D'Avino

Tutor

Prof.ssa Claudia De Lorenzo

Coordinator

Prof. Paolo Arcari

Academic Year 2014/2015

RIASSUNTO

Il carcinoma mammario è uno dei più diffusi nella popolazione femminile. L'immunoterapia, basata sull'impiego di anticorpi monoclonali diretti contro antigeni cellulari associati a tumore, rappresenta una valida strategia per il trattamento selettivo delle cellule neoplastiche. Il recettore tirosina chinasi ErbB2, iper-espresso in diversi tipi di carcinoma, tra cui quello mammario, è stato considerato uno dei bersagli più promettenti per l'immunoterapia. Sebbene Trastuzumab (Herceptin[®]), l'anticorpo umanizzato attualmente in uso clinico per la terapia del carcinoma mammario ErbB2-positivo sia efficace, può generare fenomeni di resistenza e/o cardiotossicità.

Un nuovo frammento anticorpale umano (scFv), chiamato Erbicina, è stato ottenuto nel nostro laboratorio mediante tecnologia del *phage display* e riconosce un epitopo di ErbB2 diverso da quello di Trastuzumab. Erbicina è stato fuso ad una variante della ribonucleasi pancreatica umana (HP-RNasi), resistente all'inibitore delle RNasi, in modo da ottenere una immunoRNasi (IR) anti-ErbB2 chiamata Erb-HP-DDADD-RNasi. La nuova IR è in grado di inibire la crescita di cellule di carcinoma mammario resistenti o scarsamente sensibili a Trastuzumab, sia *in vitro* che *in vivo*, più efficacemente dell'IR parentale, sensibile all'azione dell'inibitore. Inoltre, Erb-HP-DDADD-RNasi non mostra effetti cardiotossici né *in vitro* su cardiomiociti umani, né *in vivo* in modelli di topo sottoposti ad ecocardiografia prima e dopo il trattamento con la IR. Tuttavia, un'elevata percentuale di carcinomi mammari risulta caratterizzata dall'assenza di ErbB2, come quelli tripli negativi (TNBC). Pertanto, come nuovo bersaglio per l'immunoterapia del TNBC abbiamo considerato la Nucleolina (NCL), una proteina multifunzionale selettivamente espressa sulla superficie delle cellule tumorali che regola la biogenesi di alcuni microRNA coinvolti nella tumorigenesi e nella chemioresistenza. Abbiamo quindi isolato, mediante tecnologia del *phage display*, un scFv umano diretto contro la Nucleolina (NCL), chiamato 4LB5, dotato di effetti anti-tumorali selettivi.

Nel presente progetto di tesi abbiamo prodotto e caratterizzato una nuova IR umana ottenuta dalla fusione di 4LB5 con l'HP-RNasi, chiamata 4LB5-HP-RNasi. Tale IR: I) conserva l'attività enzimatica della RNasi e la capacità di legare dell'scFv parentale ad un pannello di cellule di carcinoma mammario NCL-positivo; II) riduce drasticamente e selettivamente la vitalità e la proliferazione delle stesse cellule tumorali, sia *in vitro* che *in vivo*; III) induce apoptosi e riduce i livelli di miRNA oncogenici, quali il miR-21, il -221 ed il -222.

Tali nuovi immunoagenti umani potrebbero dunque rappresentare strumenti preziosi per la terapia di carcinomi mammari che non possono essere sottoposti a trattamento con Trastuzumab, a causa di fenomeni di resistenza, cardiotossicità o mancata espressione del recettore ErbB2.

SUMMARY

Breast cancer is the most common cancer in women worldwide. A new promising anti-cancer therapy involves the use of monoclonal antibodies specific for tumor-associated antigens (TAAs). A TAA of interest for breast cancer immunotherapy is ErbB2, a tyrosine kinase receptor overexpressed in 25-30% of breast carcinomas but not on most of normal tissues.

Trastuzumab, a humanized anti-ErbB2 antibody in clinical use for the therapy of breast cancer, is effective but can cause resistance and/or cardiotoxicity. Taking advantage of phage display technology, we had previously isolated a human anti-ErbB2 scFv, named Erbicin, which recognizes an epitope different from that of Trastuzumab. We then engineered an anti-ErbB2 immunoRNase (IR), called Erb-HP-DDADD-RNase, by fusing Erbicin with a human pancreatic RNase (HP-RNase) variant, made resistant to the cytosolic RNase inhibitor (RI).

Here we report that this novel IR is endowed with antiproliferative activity for Trastuzumab-resistant breast cancer cells, both *in vitro* and *in vivo*, that is more potent than that of the parental immunoRNase, which is sensitive to the RNase inhibitor. Importantly, Erb-HP-DDADD-RNase does not show cardiotoxic effects *in vitro* on human cardiomyocytes neither impairing cardiac function in a mouse model.

Since, unfortunately, most of human breast tumors as the aggressive triple negative breast cancer (TNBC) are ErbB2-negative, we characterized a novel target for immunotherapy of TNBC to complement the promising data on IR/ErbB: Nucleolin (NCL), a multifunctional protein, selectively expressed on the surface of cancer cells, which regulates also the biogenesis of specific microRNAs (miRNAs) involved in tumor development and drug-resistance.

By using phage display, we have isolated a novel human anti-NCL scFv, named 4LB5, endowed with selective anti-tumor effects. Here we report on the construction and characterization of a novel immunoRNase made up of 4LB5 and human pancreatic RNase (HP-RNase), named 4LB5-HP-RNase. This novel IR: i) retains both the enzymatic activity of human pancreatic RNase and the specific binding of the parental scFv to a panel of surface NCL-positive breast cancer cells; ii) dramatically and selectively reduces the viability and proliferation of NCL-positive tumor cells, both *in vitro* and *in vivo*; iii) induces apoptosis and strongly affects the levels of tumorigenic miRNAs, such as miR-21, -221 and -222.

Altogether, these two novel immunoagents could be valuable tools for the therapeutic need of breast cancer patients ineligible for Trastuzumab treatment due to resistance, cardiotoxicity or lack of ErbB2 receptor.

INDEX

INTRODUCTION	1
1. <i>Breast cancer: novel ErbB2-targeted therapies</i>	1
2. <i>A novel approach for triple-negative breast cancer (TNBC) therapy</i>	5
MATERIALS AND METHODS	10
1. <i>Cell cultures</i>	10
2. <i>Antibodies</i>	10
3. <i>Bacterial strains</i>	11
4. <i>Bacterial culture medium</i>	11
5. <i>Bacterial transformation</i>	11
6. <i>Generation, expression and purification of 4LB5-HP-RNase</i>	11
7. <i>Western blotting analyses</i>	12
8. <i>RNase activity</i>	13
9. <i>Cell ELISA assays</i>	13
10. <i>Pull-down assay</i>	14
11. <i>Confocal microscopy</i>	14
12. <i>In vitro cytotoxicity assays</i>	15
13. <i>Colony Assays</i>	16
14. <i>Cellular internalization analyses</i>	16
15. <i>Purification of extracellular vesicles (EVs)</i>	17
16. <i>RNA extraction</i>	17
17. <i>Quantitative Real-Time PCRs</i>	17
18. <i>In vivo antitumor assays</i>	18
19. <i>In vivo cardiotoxicity assays</i>	19

RESULTS	20
1. <u>Breast cancer: novel ErbB2-targeted therapies</u>	20
1.1 <i>In vitro</i> cytotoxic effects on breast tumor cells and internalization of Erb-HP-DDADD-RNase.....	20
1.2 <i>In vivo</i> antitumor activity of Erb-HP-DDADD-RNase.....	22
1.3 <i>In vitro</i> effects of Erb-HP-DDADD-RNase on human cardiac cells.....	24
1.4 <i>In vivo</i> cardiotoxic effects of Erb-HP-DDADD-RNase.....	24
2. <u>A novel approach for triple-negative breast cancer (TNBC) therapy</u>	25
2.1 Generation, expression and purification of the novel anti-Nucleolin immunoRNase 4LB5-HP-RNase.....	25
2.2 Binding assays of 4LB5-HP-RNase to NCL.....	28
2.3 4LB5-HP-RNase is internalized in surface NCL-positive breast cancer cell.....	31
2.4 4LB5-HP-RNase affects cancer cell viability and proliferation <i>in vitro</i>	33
2.5 4LB5-HP-RNase induces apoptosis in surface NCL-positive cancer cells.....	35
2.6 Effects of 4LB5-HP-RNase on the levels of oncogenic intracellular and extracellular miRNAs.....	37
2.7 <i>In vivo</i> effects of 4LB5-HP-RNase.....	40
DISCUSSION	42
1. <i>Breast cancer: novel ErbB2-targeted therapies</i>	42
2. <i>A novel approach for triple-negative breast cancer (TNBC) therapy</i>	44
REFERENCES	47

List of Tables and Figures

Figure 1 - Tyrosine-kinase receptors (TKRs) of the EGFR family and ErbB2 signaling pathways.....	2
Figure 2 - Schematic representation of the phage display technology.....	3
Figure 3 - Schematic representation of the immunoRNase (IR).....	4
Figure 4 - The variant HP-RNase (HP-DDADD-RNase) and its interaction with the ribonuclease inhibitor (RI).....	5
Figure 5 - A schematic representation of the biological functions of Nucleolin in eukaryotic cells.....	7
Figure 6 - ELISA binding assay to NCL of novel fully human anti-NCL scFvs obtained by phage display and identification of 4LB5 as the best binder.....	9
Figure 7 - Characterization of anti-NCL scFv 4LB5 on breast cancer cell.....	9
Figure 8 - <i>In vitro</i> effects of the IRs on tumor cell survival.....	21
Figure 9 - Internalization of immunoRNases into tumor cells expressing different levels of ErbB2.....	22
Figure 10 - <i>In vivo</i> effects of Erb-HP-DDADD-RNase or Erb-HP-RNase on trastuzumab-resistant JIMT-1 tumors induced in mice.....	23
Figure 11 - Cardiotoxic effects of Erb-HP-DDADD-RNase <i>in vitro</i> and <i>in vivo</i>	25
Figure 12 - Schematic representation and biochemical analyses of purified 4LB5-HP-RNase.....	27
Figure 13 - ELISA binding assays of 4LB5-HP-RNase to NCL on cancer cells.....	29
Figure 14 - Binding specificity assays of 4LB5-HP-RNase to NCL.....	31
Figure 15 - 4LB5-HP-RNase is internalized in TNB cells.....	32
Figure 16 - <i>In vitro</i> effects of the immunoRNase on tumor cell survival.....	34

Figure 17 - *In vitro* effects of 4LB5-HP-RNase on cancer cell proliferation.....**35**

Fig. 18 - Effects of 4LB5-HP-RNase on cancer cell apoptosis.....**36**

Fig. 19 - Effects of 4LB5-HP-RNase on miRNAs levels in cancer cells.....**38**

Fig. 20 - Effects of 4LB5-HP-RNase on cancer cells-derived extracellular vesicles-miR-21.....**40**

Fig. 21 - *In vivo* effects of 4LB5-HP-RNase on NCL-positive tumors induced in mice by using MDA-MB-231 breast cancer cells.....**41**

INTRODUCTION

1. Breast cancer: novel ErbB2-targeted therapies

Breast cancer is the most common cancer in women worldwide with nearly 1.7 million new cases diagnosed in 2012. It affects one in eight women during their lives (1).

The treatment for patients with breast cancer is continuously evolving. Over the last decade, the introduction of novel antitumor agents has led to notable changes in therapeutic strategy, and improvements in survival, yet breast cancer remains an increasing public health problem.

One of the most promising and exciting fields in modern anti-cancer therapy involves the use of monoclonal antibodies to target tumor-associated antigens (TAAs) expressed at high levels on the surface of cancer cells but not on their normal counterpart. A large number of monoclonal antibody-based therapies is undergoing clinical evaluation or has been already approved by FDA and currently in use (2).

A TAA of interest for breast cancer immunotherapy is ErbB2 (HER-2/neu), a tyrosine kinase receptor, overexpressed on many carcinoma cells of different origin (3-5), which plays a key role in the development of malignancy and correlates with a poor prognosis (6).

Antitumor strategies based upon antibodies have been successfully established for ErbB2, leading to the recent clinical approval of humanized antibodies and immunoconjugates, such as Pertuzumab and T-DM1 (7, 8) and to the wide clinical use of Trastuzumab either in early or metastatic breast cancer (9, 10). However, the clinical efficacy of these drugs is still limited by resistance and cardiotoxicity issues. For instance, up to 70% of breast cancer patients are resistant to Trastuzumab and large-scale clinical studies have shown that 7 or 28% of patients suffer from cardiac dysfunction when Trastuzumab is used alone or in combination with anthracyclines, respectively (11-15). The underlying mechanism of Trastuzumab cardiotoxicity is based on its capacity to inhibit the neuregulin (NRG-1) mediated heterodimerization of ErbB2/ErbB4 on cardiac cells, thus interfering with the pathways of myocyte survival, induced by ErbB2 (16). ErbB2 is indeed the preferential heterodimerization partner for the other members of EGFR family.

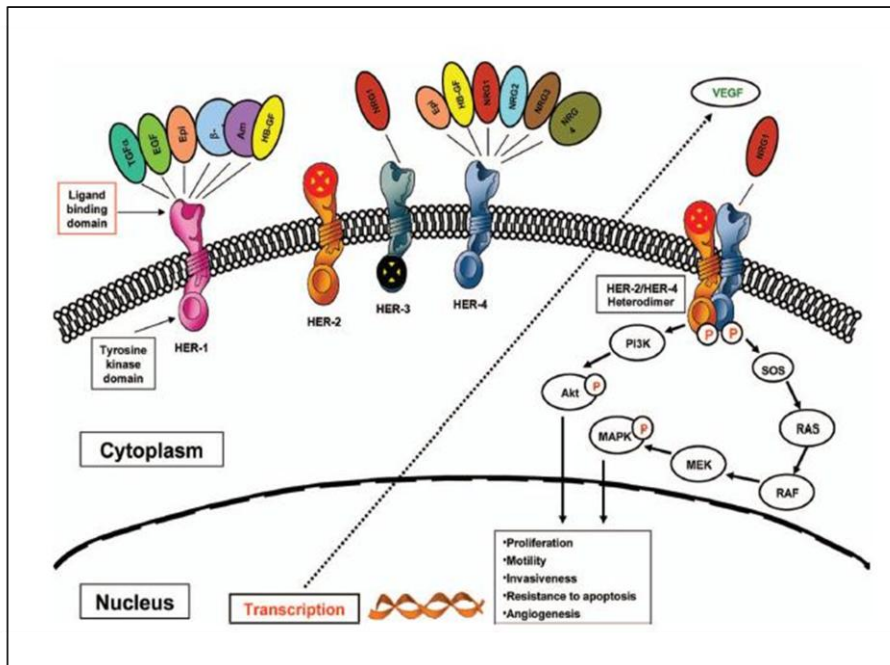


Fig. 1 - Tyrosine-kinase receptors (TKRs) of the EGFR family and ErbB2 signaling pathways.

Epidermal growth factor receptor–ligand interaction induces the heterodimerization of ErbB receptors, which in turn results in the activation of intracellular tyrosine kinase domain and downstream signaling cascades that mediate cell growth, differentiation, and survival (17-19) such as mitogen-activated protein kinase (MAPK) and phosphatidylinositol-3-kinase (PI3K) pathways (Figure 1).

The ErbB2 receptor lacks nature ligands and differently from the other ErbB receptors is already in an open conformation which can interact with the other members of the family, thus its overexpression in cancer cells induce dimerization and initiates signal transduction activating dysregulated proliferation.

Another obstacle to the success of present-day immunotherapy is represented by the immune responses against the nonhuman components. In fact an ideal anticancer drug should not only selectively target tumor cells, but it should also be nonimmunogenic.

In order to overcome these limits fully human immunoagents, obtained by phage display technology (20), capable of inhibiting tumor growth, would meet all these requisites, and provide safe and highly selective antitumor drugs.

The phage display methodology allows for the isolation of fully human antibody fragments, which are the minimal portions of an antibody still capable of binding to the target antigen (Figure 2). A single chain variable fragment (scFv) is made up of the variable domains of the heavy (VH) and light chain (VL) connected by a flexible oligopeptide. This fragment retains the binding specificity for the antigen but is able to diffuse more easily into the tumor masses.

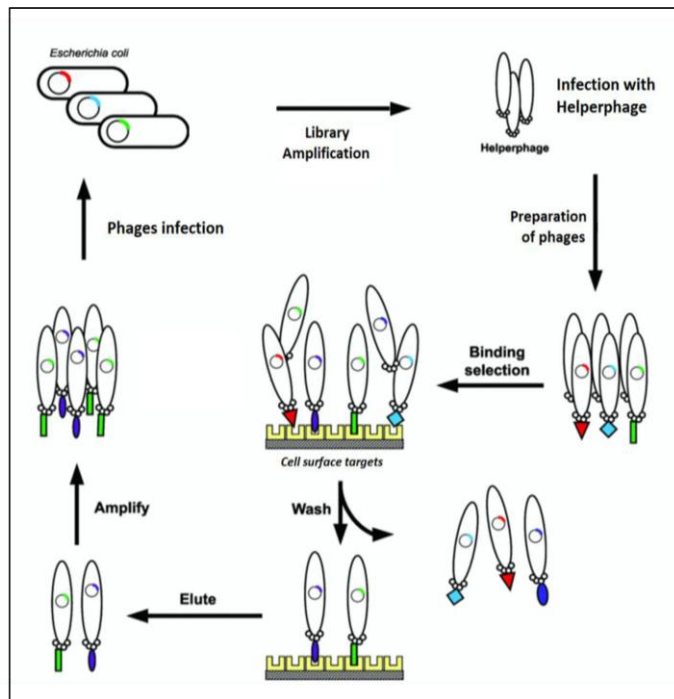


Fig. 2 - Schematic representation of the phage display technology.

These scFvs can be conjugated with radionuclides or toxins derived from plants or bacteria (21, 22), thus combining the potent toxicity of these molecules with the antigen specificity of the antibodies (23, 24) for an efficient killing of target cells.

However, these immunoconjugates, called “immunotoxins”, could be immunogenic and can induce non-specific toxicities, such as vascular leak syndrome and hepatotoxicity, thus limiting the therapeutic potential of these immunoconjugates (25, 26).

To circumvent these problems, the toxin has been replaced by a non-immunogenic and non-toxic ribonuclease, such as ribonuclease 1 or human pancreatic ribonuclease.

The novel human antitumor immunoconjugate, named immunoRNase (IR), was engineered in our laboratory by isolation through phage display technology of a novel human antibody fragment anti-ErbB2, named Erbicin (27), and its genetic fusion with a human pancreatic ribonuclease (HP-RNase) (Figure 3) (28). Erbicin binds to ErbB2 receptor and is internalized by the cells through receptor-mediated endocytosis, thus allowing for the RNase to enter the cells and act as a toxin only for target cells by exerting its enzymatic activity on cellular RNAs (28).

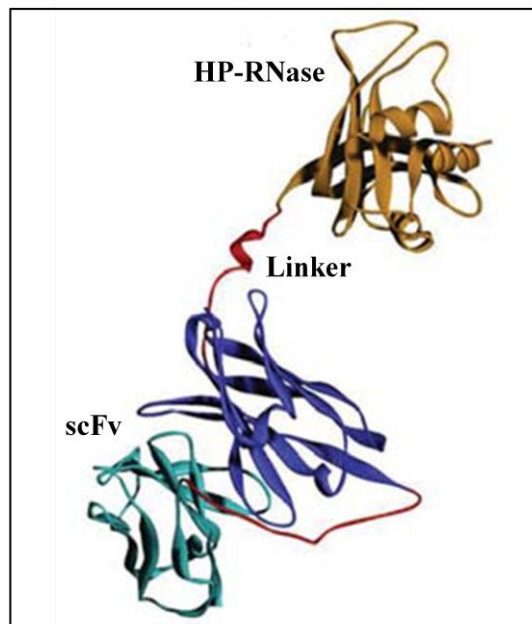


Fig. 3 - Schematic representation of the immunoRNase (IR).

This first-generation anti-ErbB2 immunoRNase (Erb-HP-RNase) binds selectively and with high affinity to ErbB2-positive cells, and specifically inhibits their proliferation both *in vitro* and *in vivo* (28-30).

Furthermore, Erb-HP-RNase does not show cardiotoxic side effects either *in vitro* or *in vivo* probably because Erbicin binds to an epitope different from that of Trastuzumab (31, 32).

Unexpectedly, however, Erb-HP-RNase was found to be at least partially sensitive to the neutralizing action of the RNase inhibitor (RI), a cytosolic protein with a high affinity for HP-RNase (33-35).

Based on the concern that the fraction of Erb-HP-RNase sequestered by the cytosolic inhibitor could not exert its antitumor

activity, we engineered a second-generation immunoRNase, named Erb-HP-DDADD-RNase, by fusing Erbicin with a variant of HP-RNase made resistant to RI. In this variant, five residues of the ribonuclease at the RI-HP-RNase interface are replaced (R39D/N67D/N88A/G89D/R91D) in order to reduce the affinity for RI but still retaining high RNA-degrading activity (35) (Figure 4). Erb-HP-DDADD-RNase has been found to be fully resistant to RI inhibition and kill mammary ErbB2-positive tumor cells more efficiently than Erb-HP-RNase (36).

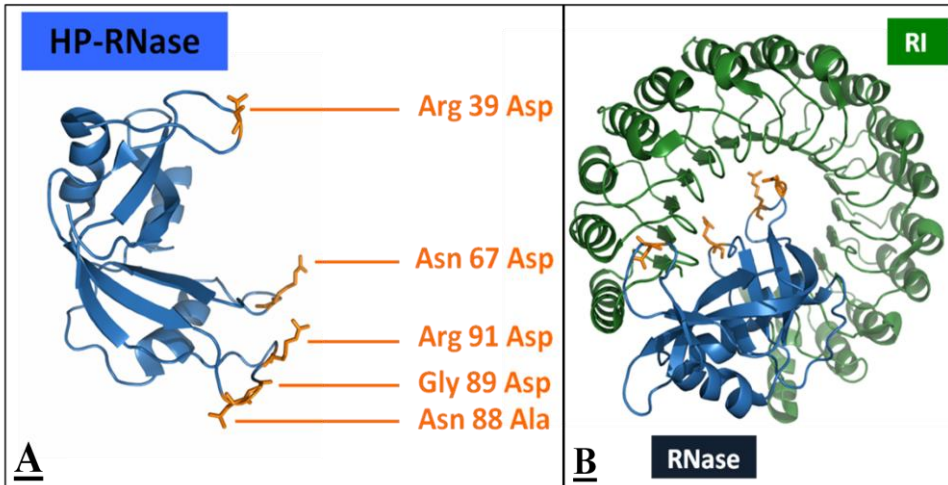


Fig. 4 - The variant HP-RNase (HP-DDADD-RNase) and its interaction with the ribonuclease inhibitor (RI). **A:** The five residues replaced in the pancreatic ribonuclease. **B:** The complex of RI and HP-RNase.

Here we report on the antitumor properties of Erb-HP-DDADD-RNase on Trastuzumab-resistant breast cancer cells and its eventual cardiotoxic effects, tested both *in vitro* and *in vivo*, to reveal its therapeutic potential for cancer patients that suffer from cardiac dysfunction and/or are ineligible for Trastuzumab treatment due to natural or acquired resistance.

2. A novel approach for triple-negative breast cancer (TNBC) therapy

Unfortunately, a high fraction of breast tumors do not express ErbB2. Since ErbB2 overexpression/amplification occurs only in ~25% of human breast cancer patients (4), new targets have been investigated for the other untreatable breast tumors, such as triple-negative breast cancer (TNBC).

TNBC is indeed characterized by the absence of estrogen receptor (ER), progesterone receptor (PR) and ErbB2, thus excluding the possibility of using efficacious targeted therapies developed against these proteins. TNBC accounts for ~14% of all breast cancers and approximately 170,000 patients worldwide are diagnosed annually with TNBC (37). These patients show high risk of recurrence and visceral metastasis and their death rate is disproportionately higher than any other subtype of breast cancer (median overall survival around 12 months in the metastatic setting) (38).

A new attractive target for triple-negative breast cancer immunotherapy is today represented by Nucleolin (NCL), a major nucleolar protein of exponentially growing eukaryotic cells (39), which is directly involved in the ribosomal processing (40, 41). Nucleolin represents a particularly important multi-functional protein which plays a key role in DNA and RNA metabolism, chromatin structure, rDNA transcription, rRNA maturation and ribosome biogenesis; it also functions as a cell surface receptor, where it acts as a shuttling protein between cytoplasm and nucleus, and thus it can even provide a mechanism for extracellular regulation of nuclear events (42, 43) (Figure 5).

Although NCL is predominantly localized in the nucleus, a large number of reports have shown enhanced expression of cytoplasmic and surface NCL in many different tumor cell types such as leukemic (44), renal (45), pulmonary (46), prostate (47), intestinal (48, 49), breast (46, 50, 51), hepatic (52), kidney (53), cervical (46, 54) and colon (46, 55) cancer cells, melanomas (46, 56) and gliomas (57, 58).

Altered NCL surface expression and localization is directly or indirectly involved in signal transduction events subsequently to its interaction with several molecules/receptors on the cell surface that are all known to be involved in tumor cell growth, invasiveness, inflammation and/or angiogenesis. In line with its role in RNA processing, recent published studies (41) report that NCL also promotes the maturation of a specific set of microRNAs (miRNAs), such as miR-21, -221 and -222, whose up-regulation is involved in breast tumorigenesis, metastasis formation, and drug resistance (59-62).

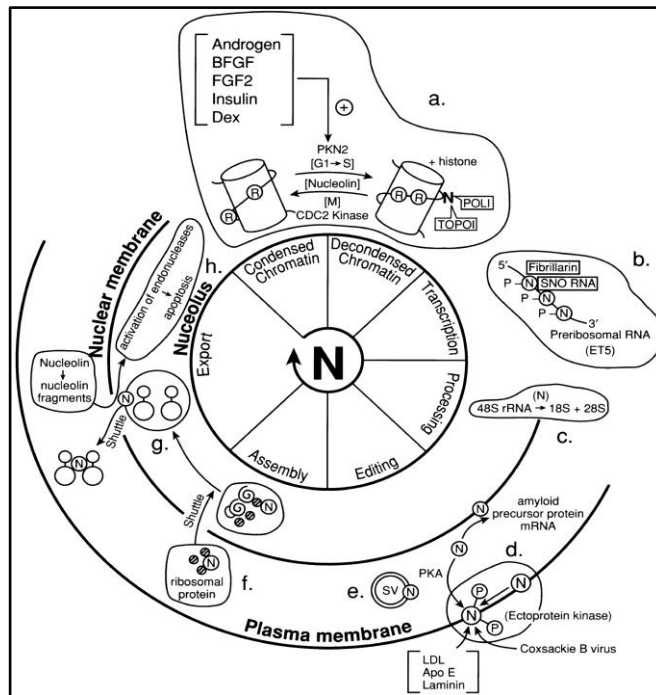


Fig. 5 - A schematic representation of the biological functions of Nucleolin in eukaryotic cells. a) chromatin condensation and decondensation; b) Nucleolin and pre-RNA; c) maturation of 48S rRNA; d) cell surface functions; e) expression of Nucleolin in small secretory vesicles; f) shuttling activities: Nucleolin acts as a shuttling protein to carry ribosomal protein from cytoplasm to nucleus during the assembly of ribosomes; g) export activities: Nucleolin might be involved in exporting the assembled ribosomes from nucleus to cytoplasm; h) cell death and apoptosis.

NCL targeting affects breast cancer aggressiveness through miRNA regulation as NCL could mediate their transfer to the cytosol, to cell membrane and to the extracellular microenvironment, thus regulating their oncogenic effects. Indeed, the cells release a significant number of RNA-binding proteins into the culture medium, such as Nucleolin and Nucleophosmin 1 (NPM1), which can protect miRNA from degradation, thus suggesting that these proteins may play a role in the exportation, packaging and protection of extracellular miRNAs (63).

Recently, the release from tumor cells of extracellular vesicles (EVs) has become the subject of increasing interest for its role in cancer intercellular communication. The EVs are spherical structures made up of a lipid bilayer that contain proteins, genetic material and bioactive lipids

(64, 65) derived from the cytosol of the donor cells, thus the cargo represents the information released by one cell to a recipient cell. The EVs include exosomes (50-100 nm) secreted from the endosomal membrane compartment after the fusion of multivesicular bodies with the plasma membrane, and microvesicles (100 nm-1 μ m), which bud directly from the plasma membrane (64). However, numerous similarities exist in terms of physical characteristics and compositions of exosomes and microvesicles, thus making challenging the exclusive purification of the target vesicles after their secretion from cells (66, 67).

A key component of the EVs-associated cargo is represented by miRNAs which can be delivered to another cell, and thus can display their oncogenic role (65).

Altogether these observations support the importance of tumorigenic miRNAs in immune escape, neovascularization and metastasis and the key role of NCL to affect their levels.

Thus surface NCL has become an attractive target for cancer therapy even because is continuously and abundantly expressed on the tumor cell surface compared with normal cells and is associated with the proliferative capacity of cells independently from nuclear NCL (68).

Several groups have attempted to develop molecules, such as aptamers (AS1411) or peptides (HB-19, V3 loop-mimicking pseudopeptide, N6L, and F3) (69-72), to bind and to inhibit NCL in cancer cells. These compounds have also been suggested as potential carriers for the targeted delivery into cancer cells of several antineoplastic agents. Although promising, aptamers and peptides targeting NCL suffer from intrinsic limitations, such as extremely short half-life, undesired immunostimulatory actions, and still unknown toxicological effects (73).

To circumvent these problems, in our laboratory, in collaboration with a research group of the Ohio State University, a novel fully human anti-NCL scFv, named 4LB5, has been isolated by phage-display technology (Figure 6) (74). This immunoagent recognizes with high affinity the RNA binding domain (RBD) of NCL, selectively binds to NCL on the cell surface and discriminates between cancer and normal-like breast cells (Figure 7). 4LB5 is also internalized into the cytoplasm of target cells, reduces their cell viability and proliferation both *in vitro* and *in vivo*, and abrogates the biogenesis of NCL-dependent miRNAs (74).

To enhance the potential therapeutic effect of 4LB5 we have engineered an anti-NCL novel fully human immunoRNase, named 4LB5-HP-RNase, by fusing 4LB5 with the human pancreatic ribonuclease in a similar manner to the previously described anti-ErbB2 IR (28).

Here we describe the production and characterization of this novel IR and we report on its antitumor effects both *in vitro* and *in vivo*.

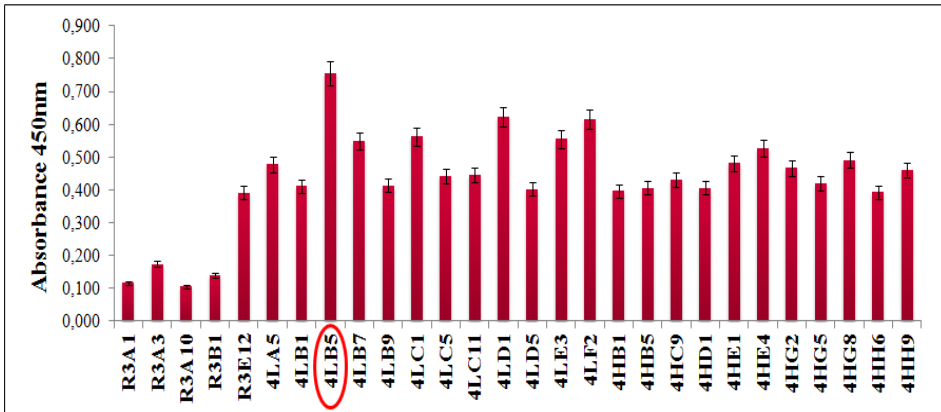


Fig. 6 - ELISA binding assay to NCL of novel fully human anti-NCL scFvs obtained by phage display and identification of 4LB5 as the best binder.

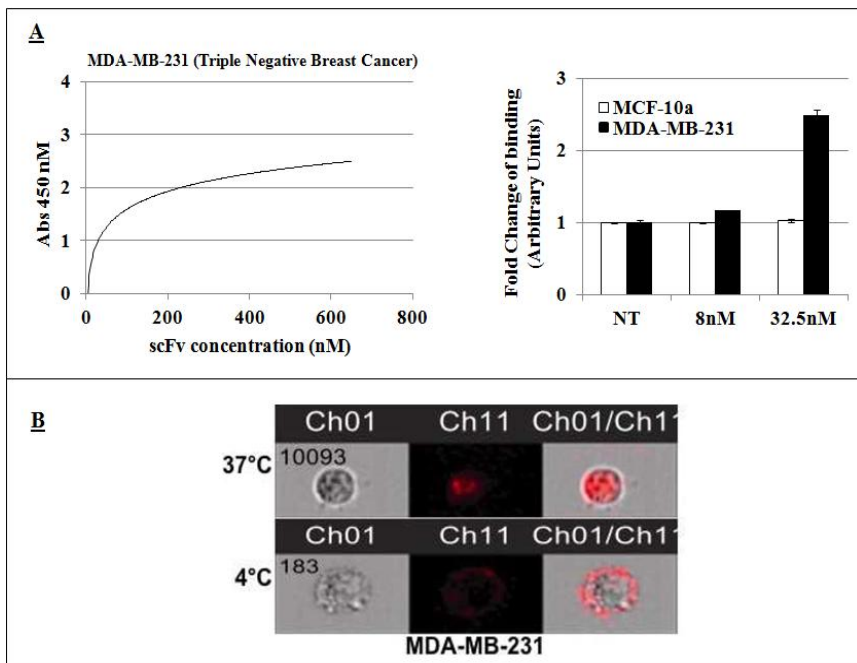


Fig. 7 - Characterization of anti-NCL scFv 4LB5 on breast cancer cells. A: Binding assays of 4LB5 to NCL-positive triple-negative breast cancer MDA-MB-231 cells or to NCL-negative breast normal-like MCF-10a cells. **B:** Internalization of Cy5 labelled 4LB5 by MDA-MB-231 cells.

MATERIALS AND METHODS

1. Cell cultures

The human breast cancer SKBR3, MDA-MB-436 and BT549, the colorectal adenocarcinoma SW-620, and the human epidermoid carcinoma A431 cell lines were cultured in RPMI 1640 (Gibco BRL, Life Technologies, Paisley, UK). The JIMT-1 cell line, established from a pleural metastasis of a 62-year-old breast cancer patient resistant to Trastuzumab, and the triple-negative breast cancer MDA-MB-231 cell line were grown in Dulbecco's modified Eagle's medium (Gibco BRL). The human breast cancer MCF-7 cell line was grown in Eagle's Minimum Essential Medium (MEM, Gibco BRL).

Media were supplemented with 10% (vol/vol) heat-inactivated fetal bovine serum (7.5% for JIMT-1), penicillin (100 UI ml^{-1}), streptomycin ($100 \mu\text{g ml}^{-1}$) and 2 mM glutamine (all from Gibco BRL) in a humidified atmosphere of 95% air and 5% CO_2 at 37°C .

The normal-like breast MCF10a cell line was cultured in Mammary Epithelial Cell Growth Medium (MEGM, Lonza, Basel, CH) supplemented with 10% FBS, bovine pituitary extract, hydrocortisone, hEGF, insulin (BulletKit, Lonza) and 100 ng/ml cholera toxin.

All cell lines were purchased from the American Type Culture Collection (ATCC).

2. Antibodies

The following antibodies were used: horseradish peroxidase (HRP)-conjugated anti-penta-His mouse monoclonal antibody (Qiagen GmnH, Hilden, Germany), affinity-isolated IgGs from a rabbit anti-HP-RNase antiserum (Igtech, Salerno, Italy), anti-NCL mouse monoclonal antibody (Santa Cruz Biotechnology, Inc., Dallas, TX, USA), anti-PARP rabbit polyclonal antibody, anti-ErbB2 rabbit monoclonal antibody (Cell Signaling Technology, Danvers, MA, USA), anti-actin rabbit polyclonal antibody (Sigma-Aldrich, St Louis, MO, USA), HRP-conjugated anti-rabbit immunoglobulins from goat antiserum, HRP-conjugated anti-mouse immunoglobulins from goat antiserum (Thermo Scientific, Rockford, IL, USA).

3. Bacterial strains

The *E. coli* DH5 α (Invitrogen, Life Technology, Inc., Paisley, UK) and BL21 DE3 (Novagen-Merk Millipore, Darmstadt, Germany) strains were used for cDNA amplification and expression of the immunoRNases, respectively.

4. Bacterial culture medium

LB (Luria-Bertani) culture medium was used for the growth of bacteria and prepared as described by Sambrook et al. (75). To transform the *E. coli* BL21 DE3 competent cells, 50 μ g/ml ampicillin (Applichem GmbH, Darmstadt, Germany) was added to the medium.

5. Bacterial transformation

The BL21 DE3 competent cells (200 μ l) were transformed with 50 ng plasmid DNA and incubated on ice for 40 min. The cells were subjected to heat shock at 42°C for 2 min and then incubated at 37°C for 1 hour after addition of 800 μ l LB medium. Aliquots of each mixture (200 μ l) were seeded on LB-agar plates containing 100 μ g/ml ampicillin, which were then incubated at 37°C for 16 h.

6. Generation, expression and purification of 4LB5-HP-RNase

The cDNA encoding the human pancreatic RNase was cloned into the T7 promoter-based *E. coli* pET22b+ expression vector downstream to the sequence encoding the available human 4LB5 scFv. A spacer was included between the two cDNAs to minimize the steric hindrance between the two moieties of the chimeric protein, as previously described (36). The recombinant plasmid was fully sequenced to confirm the expected DNA sequence.

Cultures of *Escherichia coli* BL21 DE3 (Novagen, Merk Millipore, Darmstadt, Germany), previously transformed with the recombinant pET22b+ expression vector containing the cDNA of 4LB5-HP-RNase, were grown at 37°C in Luria-Bertani (LB) medium containing 50 μ g/ml ampicillin until the exponential phase was reached. The expression of IR was induced by addition of 1 mM isopropyl- β -D-thiogalactopyranoside (IPTG; Applichem GmbH, Darmstadt, Germany) in the cell culture,

which then was grown at room temperature for 4 h. The cells were harvested by centrifugation at 6000 rpm for 15 min at 4°C.

Recombinant protein was extracted from the insoluble fraction of pET22b(+)-4LB5-HP-RNase-transformed BL21 (DE3) bacterial cells. To this aim, the fraction was solubilized in a PBS buffer containing 7 M UREA and incubated by slowly rotating overnight at 4°C in the presence of EDTA-free protease inhibitors (Roche Applied Science GmbH, Mannheim, Germany). After centrifugation at 28000 g for 20 min at 4°C the supernatant was incubated with a 100% saturated solution (4M) of ammonium sulfate, added drop-wise at 4°C, to allow for the protein precipitation. The mixture was incubated for 1 hour at 4°C while slowly stirring and then centrifuged at 28000 g for 10 min at 4°C. The precipitated material was resolubilized in resin binding buffer (20 mM sodium phosphate, 0,5 M NaCl, 10 mM imidazole pH 7.4) in the presence of 4 M UREA and EDTA-free protease inhibitors, and incubated for further 18 h at 4°C while slowly stirring. After centrifugation at 28000 g for 10 min at 4°C in order to remove insoluble proteins, the cleared supernatant was loaded on an immobilized-metal affinity chromatography (IMAC) by incubation with cobalt-chelating resin (TALON[®]; Clontech, Palo Alto, CA, USA) overnight at 4°C by gentle rotation. After extensive washes in an appropriate buffer (20 mM sodium phosphate, 0,5 M NaCl, 20 mM imidazole) by decreasing urea concentration in 10% glycerol (vol/vol), the elution step was performed with the same buffer containing a higher concentration of imidazole (250 mM).

The “BCA Protein Assay” kit (Pierce, Thermo Fisher Scientific) was used to measure the concentration of the purified protein according to the manufacturer’s recommendations. Briefly, the samples were incubated with BCA at 60°C for 30 min and the absorbance was measured spectrophotometrically at 562 nm. All measurements were performed in duplicate.

7. Western blotting analyses

The purity of the final preparation was evaluated by SDS-PAGE as described by Laemmli (76). At the end of the electrophoretic run, performed at 150 V, the gel was treated as follows:

- a) **Coomassie staining:** the gel was stained in a Coomassie blue solution (20% isopropanol, 10% acetic acid; 0,1% Coomassie blue) by

incubation for 30 min under gentle shaking. The gel was destained with extensive washes in a solution containing 20% ethanol and 7% acetic acid.

- b) **Western blotting analyses:** the proteins were transferred by electroblotting (25 V) onto a PVDF membrane at 4°C for 16 h. The membrane was incubated in 10 ml of blocking solution (1X PBS, 0,1% Tween 20, 5% BSA) at 25°C for 1 h and then incubated with appropriate dilutions of a peroxidase-conjugated anti-His antibody in PBS containing 0,1% Tween and 1% BSA at 25°C for 90 min. After extensive washes in a PBS solution containing 0,1% Tween 20, the bands were detected by chemiluminescence with a *phosphorimager* (45–710; Bio-Rad, Hercules, CA, USA).

8. *RNase activity*

RNase zymograms, carried out by SDS-PAGE electropherograms, were performed as previously described (77).

Briefly, the gel was incubated in a buffer of 50 mM Tris-HCl pH 7.4 containing 25% isopropanol solution for 30 minutes to increase the sensitivity of the signal detection. The gel was equilibrated in 50 mM Tris-HCl pH 7.4 for 30 minutes and then incubated in the same solution containing 4 mg/ml yeast RNA (Sigma-Aldrich) at 37°C for 10 min. The gel was washed out with 50 mM Tris-HCl pH 7.4 and stained in a solution of 0,2% toluidine blu containing 0,1% acetic acid solution for 15 minutes at room temperature by gentle agitation. Finally, the gel was destained by extensive washes in water.

Erb-HP-RNase was used as positive control in a parallel assay.

9. *Cell ELISA assays*

Binding assays were performed by modified enzyme-linked immunosorbent assay (ELISA), as previously described (28). ELISA assays for 4LB5-HP-RNase or 4LB5 were performed on surface NCL-positive MDA-MB-231, MDA-MB-436, BT549 or MCF-7 breast cancer cells and surface NCL-negative MCF10a normal-like breast cells.

Briefly, all the cells were harvested in non-enzymatic dissociation solution (Sigma-Aldrich), washed and transferred to U-bottom microtiter plates (2×10^5 cells per well). After blocking with PBS containing 6% bovine serum albumin (BSA), the cells were incubated in the absence or in the presence of increasing concentrations of IR in ELISA buffer

(PBS/BSA 3%) for 90 min at 25°C by gentle shaking. After centrifugation at 1200 rpm for 7 min and the removal of supernatant, cell pellets were washed twice in 200 µl of PBS buffer, resuspended in 100 µl of ELISA buffer and incubated for 1 h with a peroxidase-conjugated anti-His antibody. After 1 h, the plates were centrifuged, washed with PBS buffer and reacted with 3,3',5,5'-tetramethylbenzidine (Sigma-Aldrich). The enzymatic reaction was stopped with 1 N HCl, and the binding values were determined from the absorbance at 450 nm and reported as the mean of three determinations. The SD ($\leq 5\%$) was calculated on the basis of the results obtained in three independent experiments.

To further confirm that the observed binding was due to the specific interaction between 4LB5 and NCL on cell surface, the binding of 4LB5-HP-RNase to MDA-MB-231 cells was analyzed by ELISA assay before and after its pre-incubation with equimolar doses (50 nM) of NCL-RBD (RNA Binding Domain) recombinant protein. To this aim IR was pre-incubated for 2 hours at 4°C with NCL-RBD recombinant protein by gentle rotation and then tested on MDA-MB-231 cells as described above.

10. Pull-down assay

Pull-down experiments were performed to determine the specific interaction between 4LB5 or 4LB5-HP-RNase and cellular NCL.

With this aim subconfluent MDA-MB-231 cells were harvested and lysed. Whole-cell extracts (WCE) were obtained by using NTEN lysis buffer (150 mM NaCl, 0.2 mM EDTA, 50 mM Tris-HCl at pH 7.5, 1% [vol/vol] NP-40) containing protease inhibitors. The “BCA Protein Assay” kit (Pierce, Thermo Fisher Scientific) was used to measure the concentration of the WCEs. An aliquot of 2 mg of total protein extracts was incubated with equimolar doses (100 nM) of 4LB5 or 4LB5-HP-RNase, or with control buffer (PBS) and loaded on Ni-NTA Magnetic Agarose Beads (Qiagen) for 2 h at room temperature by continuous stirring to allow for the capture of the chimeric proteins by their His-tag.

The resin was washed out four times with 1 ml of NTEN lysis buffer containing 0.25% NP-40. The samples were boiled in 2× SDS sample buffer, run on SDS-PAGE gel, transferred to PVDF and probed with appropriate dilutions of anti-NCL or anti-His antibodies.

11. Confocal microscopy

Internalization of 4LB5-HP-RNase was assessed by confocal microscopy. 4LB5 and 4LB5-HP-RNase were Cy5-labeled using LYNX

Rapid Cy5 antibody conjugation kit (AbD Serotec), according to the manufacturer instructions. Sub-confluent MDA-MB-231 cells were seeded over a glass multi-well, treated with 1 µg/mL of Cy5-4LB5 or Cy5-4LB5-HP-RNase diluted in complete medium and cultured at 37 °C for 4 h to allow for their internalization. Cells were extensively washed with PBS and complete medium (without Cy5-labeled antibodies) was replaced, following the addition of Hoechst dye for nuclear staining. Live cell images were acquired using an Eclipse Ti-E microscope (Nikon), and z-stacks were also acquired to obtain 3D-images and further confirm internalization. Laser conditions for fluorescence acquisition were kept constant in all the experimental points. Images were processed using the NIS-Elements software (Nikon).

12. In vitro cytotoxicity assays

Cells were seeded in 96-well flat-bottom plates; SKBR3 cells at a density of 1.5×10^4 per well; A431 and JIMT-1 cells at a density of 5×10^3 per well. To test the effects of Erb-HP-RNase or Erb-HP-DDADD-RNase on cell growth, SKBR3 and A431 cells were incubated at 37°C for 72 h with the IRs (10–100 nM) in the culture medium.

JIMT-1 cells were deprived of serum for 24 h and then treated with the IRs (10–100 nM) for 72 h in medium containing 0.1% serum. Cell counts were determined in triplicate by using the trypan blue exclusion test by an Automated Cell Counter TC10 (Bio-Rad, Richmond, CA, USA). Cell survival was expressed as a percentage of viable cells in the presence of the tested proteins, with respect to untreated control cultures. The SD ($\leq 5\%$) was calculated on the basis of the results obtained in three independent experiments.

MDA-MB-231 and MDA-MB-436 cells were plated in 96-well plates at a density of 7×10^3 per well; BT-549, MCF-7 and MCF10a cells at density of 1×10^4 per well. Cells were treated with the increasing concentrations (10-100 nM) of 4LB5-HP-RNase and incubated at 37°C for 72 h. Cells counts were performed by Trypan blue excluding test. The cell survival is reported as percentage of viable cells in the presence of the protein under test with respect to control untreated cells.

In vitro cardiotoxicity assays were performed with human fetal cardiomyocytes (HFCs) as previously described (16). Briefly, to test the cardiotoxicity of Erb-HP-DDADD-RNase, HFC cells were seeded in 96-

well microtiter plates at a density of 1×10^4 cells/well, and allowed to adhere overnight. After 16 h at 37°C, the medium was replaced with medium containing Erb-HP-RNase, Erb-HP-DDADD-RNase (each at concentration of 50 or 100 nM), or Doxorubicin (0.1 or 0.25 μ M), used as a positive control. After the treatment carried out for 72 h at 37°C, cells were washed with PBS and stained with trypan blue or tested by 3-(4,5-dimethylthiazol-2-yl)-2,5-diphenyltetrazolium bromide assay for the determination of cell survival, as previously described (16). Cell survival was expressed as percent of viable cells in the presence of the drug under test with respect to control cultures grown in the absence of the drug.

Typically, cell survival values were obtained from at least three independent experiments in which five determinations were performed for each sample. Standard deviations were calculated on the basis of the results obtained from all the experiments.

13. Colony Assays

For colony assay experiments, MDA-MB-231, MDA-MB-436 or BT-549 cells (200 cells/well) were plated in 12-well plates and treated with 100 nM 4LB5-HP-RNase or 4LB5 in complete medium for 72 h. Then, cells were replenished with complete medium without chimeric proteins and allowed to grow for 7 additional days, to allow for the formation of the colonies. Cells were then fixed with 1% glutaraldehyde in PBS, stained with Crystal violet and counted.

14. Cellular internalization analyses

ErbB2-positive SKBR3 cells and JIMT1 cells resistant to Trastuzumab were seeded in 6-well flat-bottom plates at a density of 6×10^5 /well and grown at 37°C for 24 h in culture medium. After the addition of an immunoRNase at a concentration of 200 nM, cells were incubated for 2 h at 37°C. Cells were then washed extensively with a stripping solution of 50 mM glycine buffer, pH 3.0, containing NaCl (1.0 M), harvested with dissociation solution and lysed as previously described (78). Internalized Erb-HP-RNase or Erb-HP-DDADD-RNase was detected by Western blotting of cell extracts by using appropriate dilutions of the anti-HP-RNase antibody, followed by an HRP-conjugated anti-rabbit antibody. The signal intensity of the reactive bands was measured with a phosphorimager (45–710; Bio-Rad, Hercules, CA, USA).

15. Purification of extracellular vesicles (EVs)

For EVs purification SW620 cells at 80-90% confluency were washed twice with phosphate-buffered saline (PBS) and then incubated in serum-free RPMI-1640 for 24 h to avoid potential contamination from serum-derived vesicles and proteins.

Approximately 80 mL of conditioned medium were collected and cells/cell debris were removed from the cell culture supernatant by using a combination of differential centrifugation, as follows: 50 g for 20 min, 100 g for 20 min, 300 g for 10 min, 2000 g for 20 min and 2000 g for 45 min. The cell culture supernatant was recovered and further clarified by filtration through 0.22 µm filter (Millipore).

EVs were isolated by adding ExoQuick™ exosome precipitation reagent according to manufacturer's recommendations and incubated overnight at 4°C to allow for the EVs precipitation. The ExoQuick/supernatant mixture was centrifuged at 1500 g for 30 min and the supernatant was removed.

The EVs pellet was resuspended in a sterile nuclease-free PBS solution and incubated with equimolar doses of 4LB5 or 4LB5-HP-RNase (50 nM) at 37°C for 2 h or with a PBS control solution.

16. RNA extraction

The RNA extraction was performed by using “RNA clean-up and concentration” micro kit (Norgen) according to the manufacturer's instructions. Briefly, total RNA was isolated by using a phenol/guanidine-based reagent such as Trizol. After the separation of the aqueous and organic phases, the upper fraction containing the RNA was collected into an RNase-free microcentrifuge tube. One volume of 70% ethanol was added to the sample which was then mixed by vortexing. The RNA/ethanol mixture was applied onto an RNA-binding column and centrifuged at 14000 g for 1 min. The flowthrough was discarded and the column was washed three times with the appropriate provided wash solution by spinning the sample at 14000 g for 1 min. The purified RNA was eluted in RNase-free water in a final volume of 50 µl. The RNA concentration was measured spectrophotometrically at 260 nm.

17. Quantitative Real-Time PCRs

Quantitative real-time PCRs (qRT-PCRs) were performed by using the TaqMan Fast-PCR kit (Applied Biosystems) according to the

manufacturer's instructions, using the appropriate TaqMan probes for miRNA quantification, followed by detection with the 7900HT Sequence Detection System (Applied Biosystems). All reactions were performed in triplicate. Simultaneous quantification of GAPDH was used as reference for intracellular miRNA quantification. Simultaneous quantification of RNU48 was used as negative control to evaluate the potential contamination of cellular RNAs during the EVs purification procedure. The comparative cycle threshold (Ct) method for relative quantification of gene and miRNA expression (User Bulletin #2; Applied Biosystems) was used to determine miRNA expression levels.

18. *In vivo* antitumor assays

The *in vivo* antitumor activity of Erb-HP-DDADD-RNase was determined in Balb/cAnNCrIBR athymic (*nu/nu*) mice (Charles River Laboratories, Calco, Italy). Trastuzumab resistant JIMT-1 cells were suspended in sterile PBS and injected subcutaneously into mice at a density of 2×10^6 cells/mouse (Day 0). On Day 30, when tumors were clearly detectable, Erb-HP-RNase or Erb-HP-DDADD-RNase was administered intraperitoneally five times at 72-h intervals to groups of 5 mice at doses of 1.2 mg kg^{-1} of body weight. Another group of control mice was treated with identical volumes of sterile PBS to monitor tumor development. Tumor volume (V) was calculated by the formula of a rotational ellipsoid: $V = A \times B^2$, where A is the axial diameter and B is the rotational diameter as measured with a caliper.

To test the *in vivo* activity of 4LB5-HP-RNase, 2×10^6 viable Luc+ MDA-MB-231 cells were injected into the fourth left-side mammary fat pad of female NOD-SCID mice (NOD/ShiLtSz; Charles River). Three days or 2 weeks after tumor cell inoculation, mice were treated twice a week with intraperitoneal injections of 4LB5, 4LB5-HP-RNase (each 2 mg/kg) or control buffer (PBS). Tumor size was assessed every 7 days by bioluminescence imaging, as follows. Briefly, mice were injected with 75 mg/kg Luciferin (Xenogen), and tumor growth was detected by bioluminescence at 20 min after the injection. The homebuilt bioluminescence system used an electron multiplying charge-coupled device (IVIS-200, Perkin-Elmer) with an exposure time of 30 s and an electron multiplication gain of 500 voltage gain \times 200, 5-by-5 binning, and with background subtraction. After 4 wk of treatment, mice were analyzed by bioluminescence images and then sacrificed. The tumor size was measured by using a caliper, and the volume was calculated by using the formula $L \times W \times H$.

19. *In vivo* cardiotoxicity assays

Cardiac function *in vivo* was assessed by transthoracic echocardiography in sedated 7-week-old WT C57Bl/6 mice (Harlan Italy, San Piero al Natisone, UD, Italy) by using a Vevo 2100 high-resolution imaging system (40-MHz transducer, VisualSonics, Toronto, ON, Canada). Cardiac function was evaluated by non-invasive echocardiography in basal conditions and after intraperitoneal treatment with five doses (1.2 mg kg⁻¹ of body weight) of the novel immunoRNase Erb-HP-DDADD-RNase.

Fractional shortening (FS) and radial strain (RS) were evaluated as described previously (16); ejection fraction (%EF) was calculated with the formula: %EF = (VTD–VTS/VTD) × 100. Data were the mean ± SD.

The experiments with mice described herein were conducted in accordance with the Italian regulation for experimentation on animals. All experiments *in vivo* were carried out after ethical committee approval and met the standards required by the Directive 2010/63/EU of the European Parliament.

RESULTS

1. Breast cancer: ErbB2-targeted therapies

1.1. In vitro cytotoxic effects on breast tumor cells and internalization of Erb-HP-DDADD-RNase

The novel immunoRNase Erb-HP-DDADD-RNase was tested for its cytotoxic effects on ErbB2-positive and ErbB2-negative tumor cells. The cells were plated in the absence or in the presence of increasing concentrations of the IRs, Erb-HP-RNase or Erb-HP-DDADD-RNase. After 72 h of incubation at 37°C, cell survival was measured by counting trypan blue-excluding cells. As shown in Figure 8A, Erb-HP-DDADD-RNase was found to be selectively cytotoxic in a dose-dependent manner on the ErbB2-positive SKBR3 and Trastuzumab-resistant JIMT-1 breast cancer cell lines tested, whereas no effects on ErbB2-negative A431 epidermoid cancer cells, used as control, were observed. Surprisingly, despite the different sensitivity to ribonuclease inhibitor (RI) of the two IRs, no different effects on cell survival were detected when Erb-HP-RNase or Erb-HP-DDADD-RNase were tested on SKBR3 cells expressing high levels of ErbB2, whereas a stronger cytotoxicity of Erb-HP-DDADD-RNase with respect to that of ERBrb-HP-RNase was evidenced on JIMT-1 cell line, particularly when low protein concentrations were used (79).

The different efficacy of the two immunoRNases is consistent with the hypothesis that increased levels of ErbB2 receptor lead to increased internalization. To investigate whether SKBR3 and JIMT-1 cells express different level of ErbB2 on their surface, a quantitative analysis was performed on their lysates by western blotting with a commercial anti-ErbB2 mAb (Figure 8B). The positive bands were analyzed with a phosphorimager, and the corresponding signal intensities were normalized to those obtained in the same lysates by an anti-actin antibody. Indeed, SKBR3 cells were found to express higher levels of ErbB2 with respect to JIMT-1, as expected.

Thus, SKBR3 cells expressing high levels of ErbB2 receptor allow for the internalization of large amounts of the immunoRNases that exceed the quantity of endogeneous RI, leading to the inhibition of only a small fraction of each immunoRNase (80). In contrast, lower levels of ErbB2

such as those detected in JIMT-1 cells allow for less efficient internalization of the immunoRNases, leading to a different behavior.

In these cells, Erb-HP-RNase is efficiently inhibited by RI and manifests poor cytotoxic activity, whereas the RI-resistant Erb-HP-DDADD-RNase can fully exert its activity.

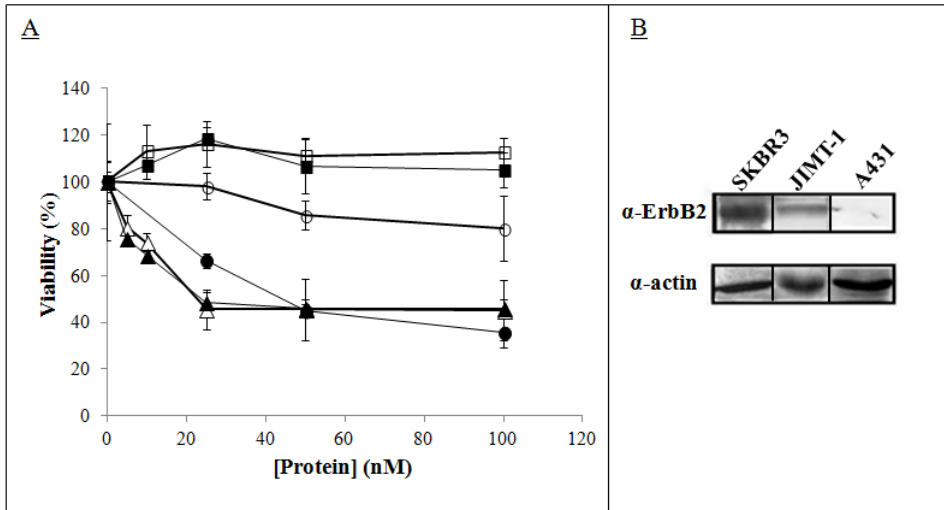


Fig. 8 - *In vitro* effects of the IRs on tumor cell survival. **A:** Dose-response curves of ErbB2-positive SKBR3 (triangles), Trastuzumab-resistant JIMT-1 (circles) cells and ErbB2-negative A431 (squares) cells, treated for 72 h with Erb-HP-RNase (empty symbols) or Erb-HP-DDADD-RNase (black symbols). **B:** Quantitative analysis by western blotting of ErbB2-receptor levels on breast cancer (SKBR3 and JIMT-1) cell lines. The A431 cell line from human epidermoid carcinoma was used as a negative control.

To test this hypothesis, an internalization assay was performed by using SKBR3 cells expressing high levels of ErbB2 and JIMT-1 cells expressing low levels of the receptor, as described in the “Materials and Methods” section. Briefly, cells were incubated for 2 h at 37°C with Erb-HP-DDADD-RNase or the parental Erb-HP-RNase, washed with low pH stripping buffer to remove the protein bound to the cell surface, lysed and analyzed by western blotting by using a rabbit anti-HP-RNase antibody, followed by a HRP-conjugated anti-rabbit antibody. The results are shown in Figure 9: the presence of a reactive band corresponding to the expected molecular weight of the immunoRNase (46 kDa) in both the lysates shows that Erb-HP-DDADD-RNase is internalized by ErbB2-

positive cells, and its levels are comparable to those of the native immunoRNase. Still, as expected, the levels of both internalized immunoRNases in SKBR3 cells are higher than those detected in JIMT-1 cells (79).

This result is in line with the hypothesis that higher levels of ErbB2 in SKBR3 cells allow for the internalization of the immunoRNases at higher levels than those detected in resistant JIMT-1 cells expressing lower levels of ErbB2.

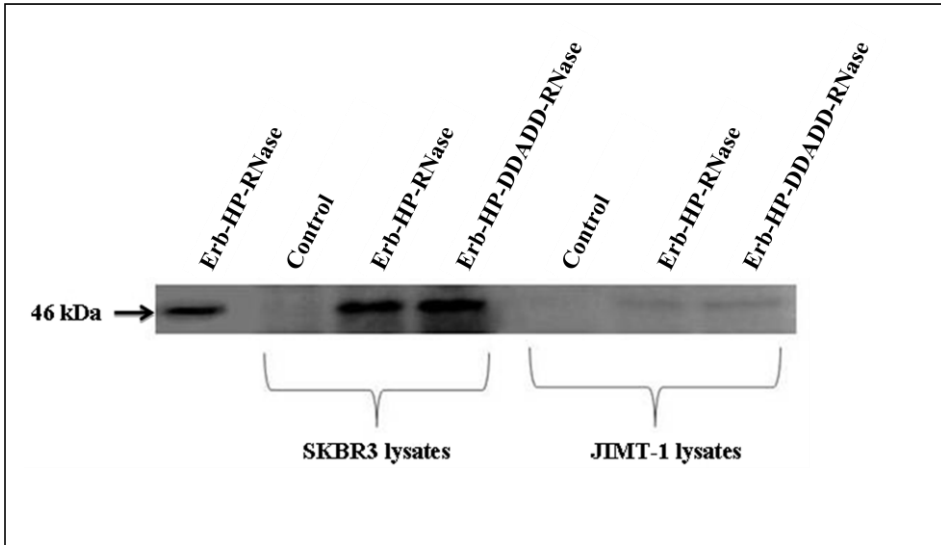


Fig. 9 - Internalization of immunoRNases into tumor cells expressing different levels of ErbB2. Analysis by Western blotting of lysates from SKBR3 cells, expressing high levels of ErbB2, or JIMT-1 cells expressing low levels of ErbB2, untreated (control) or treated with Erb-HP-RNase or Erb-HP-DDADD-RNase.

1.2. *In vivo* antitumor activity of Erb-HP-DDADD-RNase

To evaluate the *in vivo* antitumor effects of Erb-HP-DDADD-RNase, ErbB2-positive JIMT-1 cells, clinically resistant to Trastuzumab, were injected subcutaneously into Balb/cAnNCrIBR athymic (*nu/nu*) mice for *in vivo* studies. In order to compare the *in vivo* antitumor efficacy of this novel IR with that of the parental Erb-HP-RNase, the effects of equimolar doses of Erb-HP-RNase were tested in parallel on the same experimental model.

As shown in Figure 10, the treatment of mice bearing JIMT-1 tumors with 5 doses, at 72 h intervals, of 1.2 mg kg⁻¹ of Erb-HP-DDADD-RNase significantly reduces tumor volume with respect to control mice treated with a PBS solution, whereas Erb-HP-RNase has a lesser antitumor effect.

Thus, we can conclude that Erb-HP-DDADD-RNase exerts specific antitumor activity *in vivo* that is stronger than that of the parental immunoRNase, consistent with its resistance to RI (79).

During treatment, the mice did not show signs of wasting or other visible signs of toxicity, thus confirming the lack of side toxic effects for the immunoRNases.

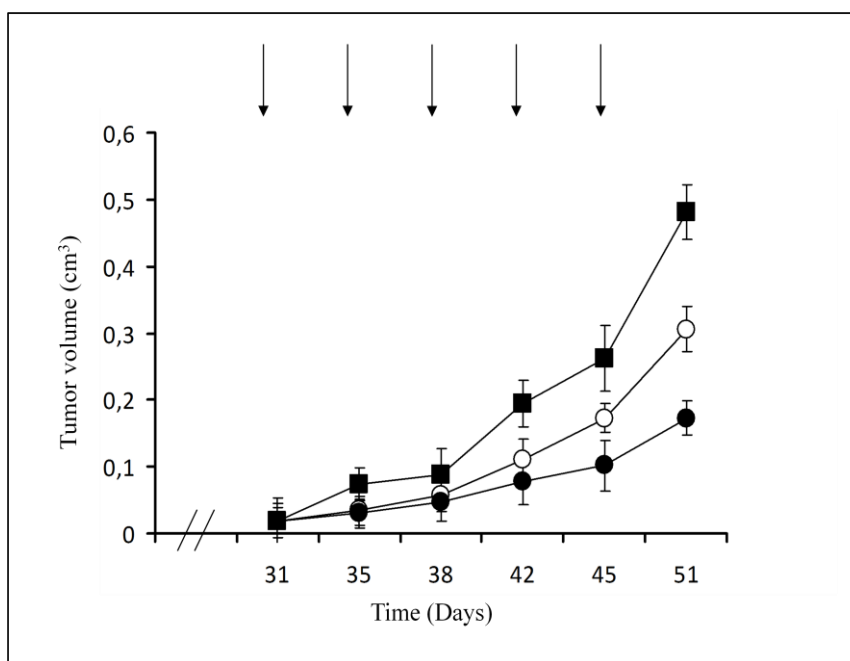


Fig. 10 - *In vivo* effects of Erb-HP-DDADD-RNase or Erb-HP-RNase on Trastuzumab-resistant JIMT-1 tumors induced in mice. Treated mice ($n = 5$) were injected with five doses (arrows; 1.2 mg kg⁻¹ of body weight) of Erb-HP-RNase (empty circles) or Erb-HP-DDADD-RNase (black circles). Control mice ($n = 5$) were treated with sterile PBS (squares).

1.3. In vitro effects of Erb-HP-DDADD-RNase on human cardiac cells

Anti-ErbB2 antibodies such as Trastuzumab have been found to be cardiotoxic in a high percentage of cases. To evaluate the potential cardiotoxic effects of Erb-HP-DDADD-RNase, a first analysis was carried out *in vitro* on human fetal cardiomyocytes (CFH). Cells were incubated at 37°C for 72 h in the absence or presence of increasing concentrations (50–100 nM) of an immunoRNase, and then analyzed by MTT assay to evaluate cell viability. Doxorubicin, at a concentration of 0.1 or 0.25 µM, was used as a positive control. As shown in Figure 11A, Erb-HP-RNase and Erb-HP-DDADD-RNase do not have cardiotoxic effects, whereas doxorubicin was toxic for cardiac cells, as expected (79).

1.4. In vivo cardiotoxic effects of Erb-HP-DDADD-RNase

The cardiotoxic effects of Erb-HP-DDADD-RNase were also tested *in vivo* on a mouse model. Groups of five mice were treated with five doses of immunoRNase comparable to those used for testing its therapeutic effects. Ecocardiography measurements were performed on mouse hearts before and after treatment. As shown in Figure 11 (B and D) Erb-HP-DDADD-RNase did not alter LVEDD and LVESD dimensions so that FS and the EF, which can signal myocardial failure, were not affected. This result is in line with the results previously obtained for the parental immunoRNase, which (unlike Trastuzumab and Doxorubicin) did not show cardiotoxic effects (31).

To further validate this finding, we evaluated as an index of myocardial deformation, the RS, which is an early and sensitive predictor of the onset of cardiac dysfunction. As shown in Figure 11C, RS was not reduced by the treatment with Erb-HP-DDADD-RNase compared with sham, thus confirming that this immunoRNase, unlike Trastuzumab (31), does not impair cardiac function (79).

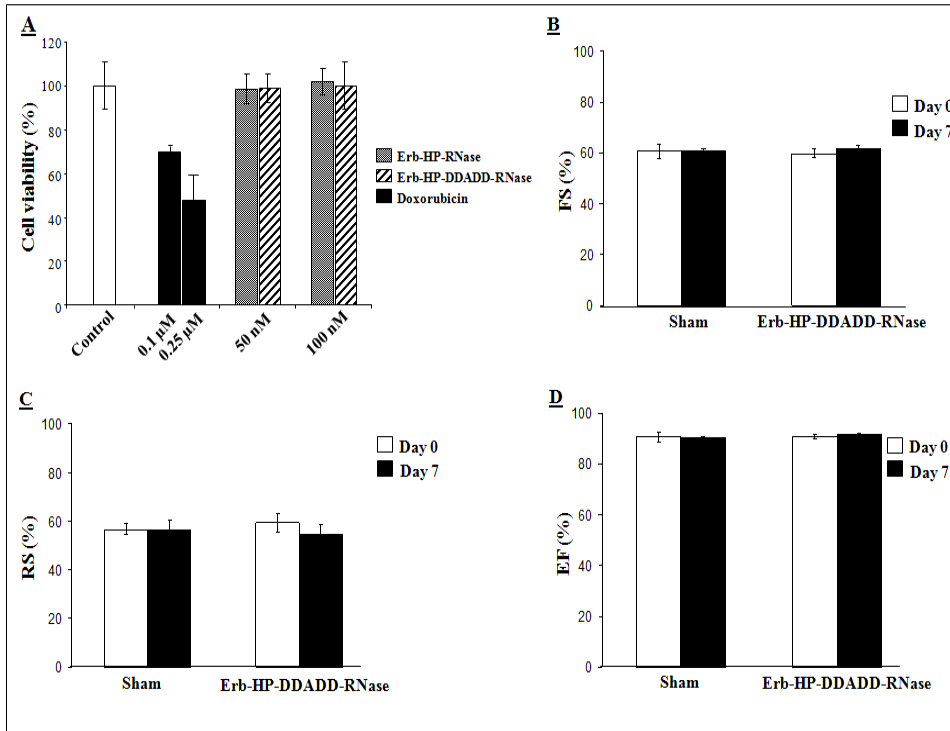


Fig. 11 - Cardiotoxic effects of Erb-HP-DDADD-RNase *in vitro* and *in vivo*. (A) Effects of Erb-HP-DDADD-RNase on the viability of human fetal cardiomyocytes (HFC) *in vitro*. Cells were treated for 72 h with Erb-HP-DDADD-RNase (striped bars) or Erb-HP-RNase (grey bars) at concentrations of 50 and 100 nM, or treated with doxorubicin (black bars) at concentrations of 0.1 and 0.25 μ M or untreated (negative control, white bars). (B–D) Effects of Erb-HP-DDADD-RNase on heart function *in vivo*. Relative FS, RS and EF are reported before and after the treatment of mice ($n = 5$) with Erb-HP-DDADD-RNase (5 doses of 1.2 mg kg⁻¹ of body weight over 7 days).

2. A novel approach for triple-negative breast cancer (TNBC) therapy

2.1. Generation, expression and purification of the novel anti-Nucleolin immunoRNase 4LB5-HP-RNase

The chimeric construct encoding 4LB5-HP-RNase was obtained by fusing the cDNAs encoding the human pancreatic RNase (HP-RNase) and the anti-NCL scFv 4LB5, as follows: the cDNA encoding the RNase was

cloned into the T7 promoter-based *E. coli* expression vector (pET22b+) downstream to the sequence encoding 4LB5 scFv. A spacer was included between the two cDNAs to minimize the steric hindrance between the two moieties of the chimeric protein, as previously described (36). The recombinant plasmid was sequenced to confirm faithful cloning. The resulting construct has the scFv at the N-terminal end, followed by a spacer inserted between the antibody fragment and the ribonuclease which is at the C-terminal end, followed by a hexahistidine tag useful for detection and purification of the chimeric construct (see Figure 12A).

For the expression, cultures of *E. coli* BL21 (DE3) transformed with the recombinant pET22b+ expression vector containing the cDNA of 4LB5-HP-RNase, were grown in LB medium with ampicillin to an OD₆₀₀ of 0.6, induced with IPTG and incubated at 25°C overnight by shaking. To verify whether the chimeric protein was expressed as a soluble protein in the periplasmic space, cells were harvested by centrifugation and resuspended in B-PER buffer to evaluate the protein expression both in the periplasmic extract and in the inclusion bodies by Western Blotting with an anti-His mAb. The recombinant protein was more abundant in the inclusion bodies, (data not shown) thus the chimeric construct was purified from the insoluble fraction of transformed BL21(DE3) bacterial cells. Briefly, the insoluble fraction was treated with 7 M UREA and then precipitated with ammonium sulfate, as described in “Material and Methods”. The resulting pellet was resolubilized in TALON binding buffer in the presence of 4 M UREA and protease inhibitors and loaded on a cobalt-chelating resin to allow for the protein purification by Immobilized-Metal Affinity Chromatography.

The protein, eluted in a high concentration imidazole buffer, was analyzed by SDS-PAGE followed by Coomassie staining. As shown in Figure 12B, a single band of the expected molecular size of about 46 kDa was detectable, thus indicating that the heterologous protein was successfully purified. By Western Blotting analyses with an anti-His antibody, a band of the expected size corresponding to the chimeric protein was visualized, thus confirming the immunoreactivity of the isolated protein (Figure 12C). The fusion protein was then tested for its enzymatic activity by a zymogram, developed by using yeast RNA as a substrate. As illustrated in Figure 12D, a single active band was detected, corresponding to the molecular weight of 4LB5-HP-RNase, thus indicating that the immunoRNase retains the enzymatic activity of native human pancreatic ribonuclease comparable to that of another immunoRNase, Erb-HP-RNase, previously described (28), used as positive control.

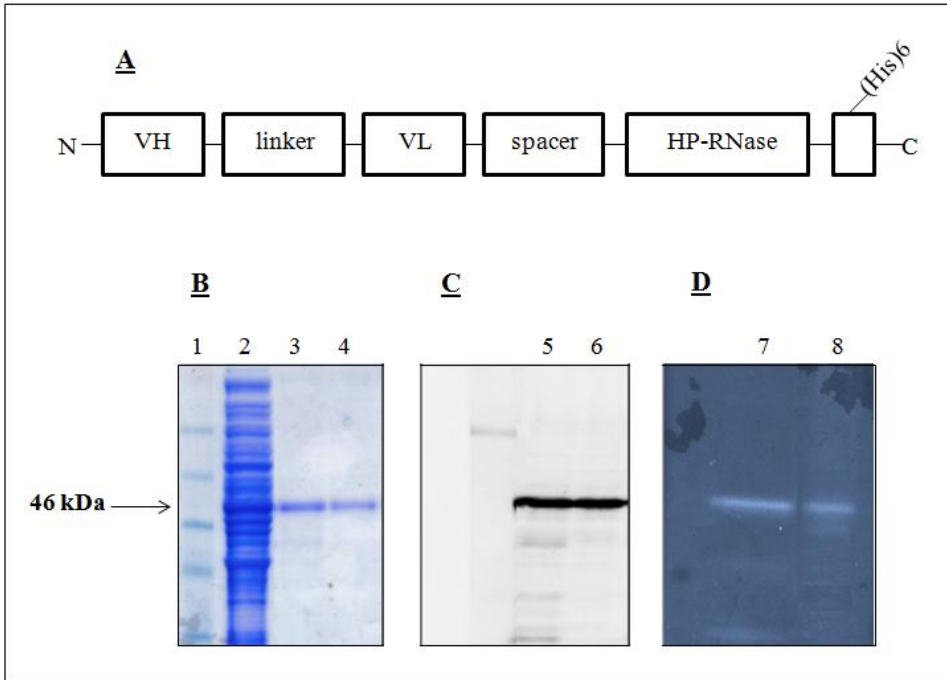


Fig. 12 - Schematic representation and biochemical analyses of purified 4LB5-HP-RNase. **A:** Schematic representation of the human anti-Nucleolin immunoRNase 4LB5-HP-RNase. VH and VL, the variable heavy and light chains of the anti-Nucleolin scFv; linker, the flexible oligopeptide conjugating VH and VL; spacer, the peptide connecting the scFv and RNase; HP-RNase, human pancreatic RNase. **B:** SDS-PAGE analysis followed by Coomassie staining of the samples eluted by IMAC. *Lane 1*, molecular weight standard; *lane 2*, flow through; *lane 3* and *4*, fractions eluted from the column. **C:** Western blotting analysis by using an anti-His antibody of the samples as in *Lane 3* and *4*, respectively. **D:** Zymogram of 4LB5-HP-RNase (*Lane 8*) using yeast RNA as a substrate; *Lane 7*, enzymatic activity of Erb-HP-RNase used as positive control of the native human pancreatic ribonuclease activity.

2.2. Binding assays of 4LB5-HP-RNase to NCL

Although NCL is predominantly localized in the nucleolus, a large number of reports have shown an enhanced expression of cytoplasmic and surface NCL in many different actively proliferating tumor cell types (40).

The ability of the recombinant fusion protein 4LB5-HP-RNase to bind to NCL-positive cells was analyzed by ELISA assays performed on a panel of breast cancer cells, such as MDA-MB-231, MDA-MB-436, BT-549 (triple negative breast cancer) and MCF7 cells (luminal epithelial breast cancer), expressing high levels of surface-NCL. In parallel assays normal-like MCF10a breast cells, expressing low levels of surface-NCL, were used as a negative control.

As shown in Figure 13A, 4LB5-HP-RNase specifically binds to all NCL-positive cancer cell lines with an affinity comparable to that of the parental 4LB5 scFv, tested in a parallel assay, whereas no significant binding to normal-like breast cells was detected. To further measure the binding affinity of 4LB5-HP-RNase to NCL expressed on live cells, binding curves were performed on each cell line by using increasing concentrations (5-500 nM) of the purified immunoRNase. As shown in Figure 13B, 4LB5-HP-RNase efficiently binds to the surface of these cells with an apparent affinity in the nanomolar range (5-50 nM).

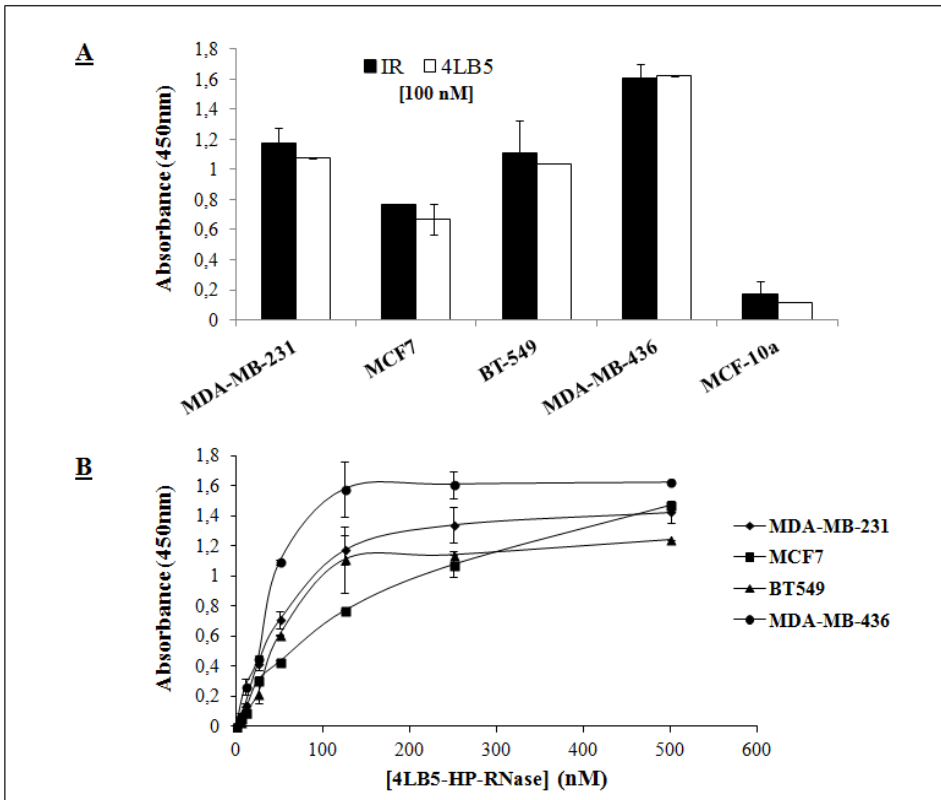


Fig. 13 - ELISA binding assays of 4LB5-HP-RNase to NCL on cancer cells. **A:** The binding of 4LB5-HP-RNase to NCL-positive MDA-MB-231, MCF-7, BT-549 or MDA-MB-436 breast cancer cells or to NCL-negative MCF10a normal-like breast cells was tested by incubating the chimeric protein (100 nM) with the cells; 4LB5 was tested at equimolar doses as a positive control in parallel assays. **B:** Binding curves of 4LB5-HP-RNase to surface NCL-positive MDA-MB-231 (rhomboids), MCF-7 (squares), BT-549 (triangles), MDA-MB-436 (circles) breast cancer cell lines performed by using increasing concentrations (5-500 nM) of the immunoRNase. All the experiments are representative of three independent experiments performed in triplicate. Mean \pm SD is reported.

To confirm that the observed binding was due to the specific interaction between 4LB5 and NCL, the binding of 4LB5-HP-RNase to MDA-MB-231 cells was analyzed by ELISA assay before and after its pre-incubation with equimolar doses of NCL-RBD (RNA Binding Domain) recombinant protein, used as a bait for the initial identification of 4LB5 scFv (74). As shown in Figure 14A, the pre-incubation of 4LB5-

HP-RNase with the NCL-RBD recombinant protein resulted in a significant reduction (over 50%) of 4LB5-HP-RNase binding to the cells with respect to that observed in the absence of the recombinant protein.

Finally, to confirm the interaction between endogenous Nucleolin and 4LB5-HP-RNase, a pull-down assay was carried out. To this aim, total cell extracts of MDA-MB-231 cells were incubated in the presence of either 4LB5-HP-RNase or 4LB5 and loaded on a high-capacity Ni-NTA resin to allow for the isolation of the protein complexes by His-tag binding of the chimeric construct, as described in “Material and Methods”. Briefly, the resin was washed with cell lysis buffer and the associated proteins were resolved by SDS-PAGE in denaturing conditions. Bound NCL trapped in immunocomplexes with 4LB5-HP-RNase or 4LB5 was detected by immunoblotting by using a commercial available anti-NCL mAb as primary antibody.

As shown in Figure 14B, immunoblotting by using an anti-His antibody confirmed similar pull-down of 4LB5-HP-RNase (46 kDa) or 4LB5 (27 kDa) proteins. Immunoreactive bands of the expected molecular size corresponding to Nucleolin (100 kDa) were observed in total cell extracts following NCL pull-down by using either 4LB5-HP-RNase or 4LB5 with comparable intensity, thus confirming that 4LB5-HP-RNase specifically binds to Nucleolin in a similar manner to the parental 4LB5 scFv.

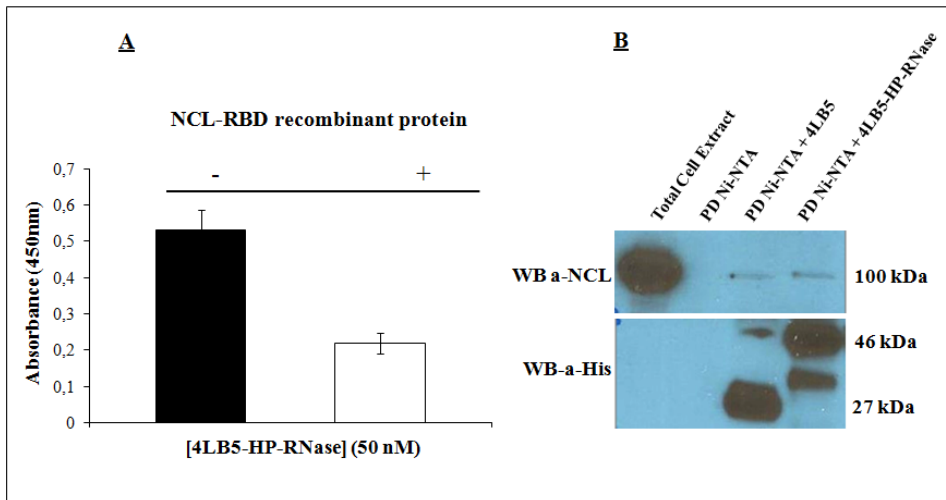


Fig. 14 - Binding specificity assays of 4LB5-HP-RNase to NCL. **A:** ELISA assay performed by testing 4LB5-HP-RNase (50 nM) on MDA-MB-231 breast cancer cells in the absence (black) or in the presence (white) of equimolar doses of NCL-RBD recombinant protein. All the experiments are representative of three independent experiments performed in triplicate. Mean \pm SD is reported. **B:** Pull-down assay performed on lysates of MDA-MB-231 cells. *Lane 1:* untreated total cell extract; *lane 2:* Ni-NTA resin (negative control); *lane 3 and 4:* cell extracts incubated with 100 nM 4LB5 or 4LB5-HP-RNase, respectively and pulled-down by using Nickel resin. Anti-NCL antibody (upper panel) and anti-His antibody (lower panel) were used to visualize the effective pull-down of endogenous NCL in the presence of either 4LB5 or 4LB5-HP-RNase.

2.3 4LB5-HP-RNase is internalized in surface NCL-positive breast cancer cells

We have previously demonstrated that, following interaction with NCL, 4LB5 is actively internalized into breast cancer cells (74). To verify whether it occurs also for 4LB5-HP-RNase, we performed internalization experiments using MDA-MB-231 TNBC cells. To this aim, 4LB5-HP-RNase was *in vitro* labeled with Cy5 fluorescent dye and added to culture medium for 4 h at 37°C. As control, cells were also incubated with 4LB5-Cy5 or with Cy5 alone, for background evaluation. Cells were extensively washed using PBS and culture medium was replaced with fresh medium

containing Hoechst for nuclear staining, and analyzed by confocal microscopy. As shown in Figure 15A, no Cy5 fluorescent signal was observed when the cells were incubated in the presence of unconjugated fluorescent dye. However, intracellular localization was observed for both 4LB5-Cy5 (Figure 15B) and 4LB5-HP-RNase-Cy5 (Figure 15C). Tri-dimensional images (z-stacks) were also acquired in order to confirm that the fluorescent signal was localized inside the cell and not on the cell surface (Figure 15D).

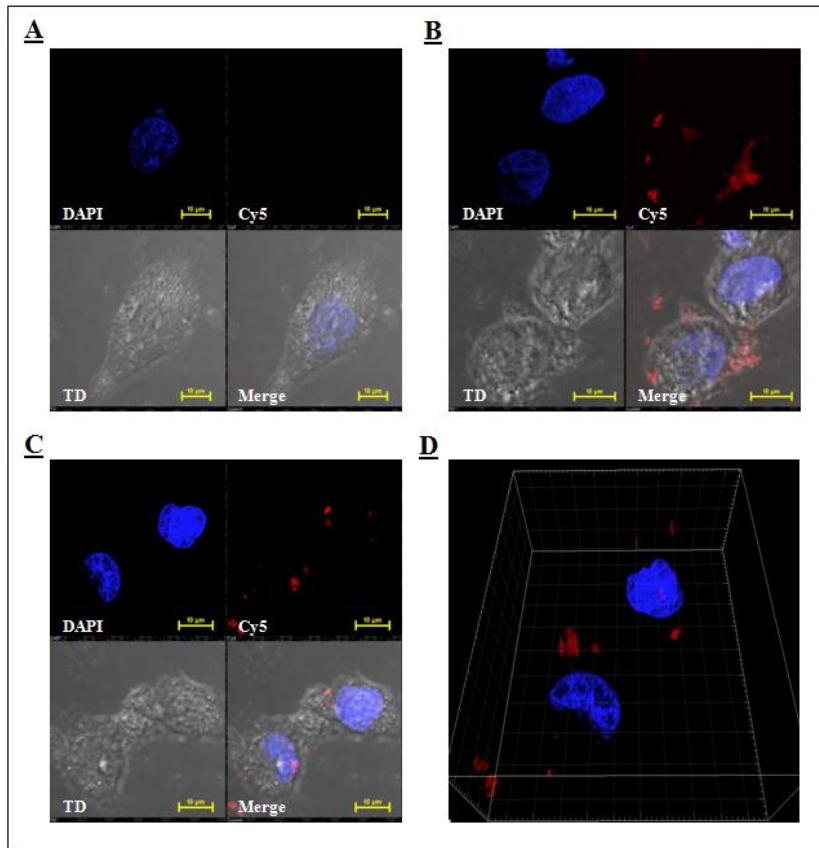


Fig. 15 - 4LB5-HP-RNase is internalized in TNBC cells. **A-C:** MDA-MB-231 cells were cultured in the presence of Cy5 (A), 4LB5-Cy5 (B) or 4LB5-HP-RNase-Cy5 (C) for 4 h. Labeled compounds not internalized were washed away and cells were incubated with Hoechst nuclear staining, and live cell images were acquired. For each experimental condition, Hoechst, Cy5, Transmitted Detector (TD) and merge is reported. **D:** 3D-reconstruction of 4LB5-HP-RNase localization. Z-stack of cells shown in Figure 4C is reported, to evaluate the intracellular localization of 4LB5-HP-RNase.

2.4 4LB5-HP-RNase affects cancer cell viability and proliferation in vitro

Down-regulation of NCL by siRNA in human cells results in growth arrest and defective centrosome duplication and appears to affect the integrity of the mitotic spindle, indicating its role in cell cycle regulation and cytokinesis (81-83). Moreover, NCL inhibition by using anti-NCL aptamer AS1411 (41) or scFv 4LB5 (74) impairs breast cancer cell proliferation both *in vitro* and *in vivo*. Then we hypothesized that the novel anti-NCL immunoRNase could display enhanced inhibitory effects, combining the anti-neoplastic properties of both 4LB5 and HP-RNase following intracytoplasmic delivery.

The ability of 4LB5–HP-RNase to display a specific cytotoxic effect on NCL-positive cells was assessed by incubating MDA-MB-231, MDA-MB-436, BT-549 or MCF7 breast cancer cells in the absence or in the presence of increasing concentrations of the protein (10-200 nM). After 72 h of incubation at 37°C, cell survival was measured by counting trypan blue-excluding cells.

As shown in Figure 16, 4LB5–HP-RNase was found to selectively and significantly inhibit the cell viability of all the NCL-positive MDA-MB-231, MDA-MB-436, BT-549 and MCF7-cell lines tested, in a dose-dependent manner, with an IC₅₀ of about 25 nM, 50 nM, 12,5 nM or 25 nM, respectively, whereas only slight effects on NCL-negative MCF-10a (normal-like) breast control cells were observed at high concentrations.

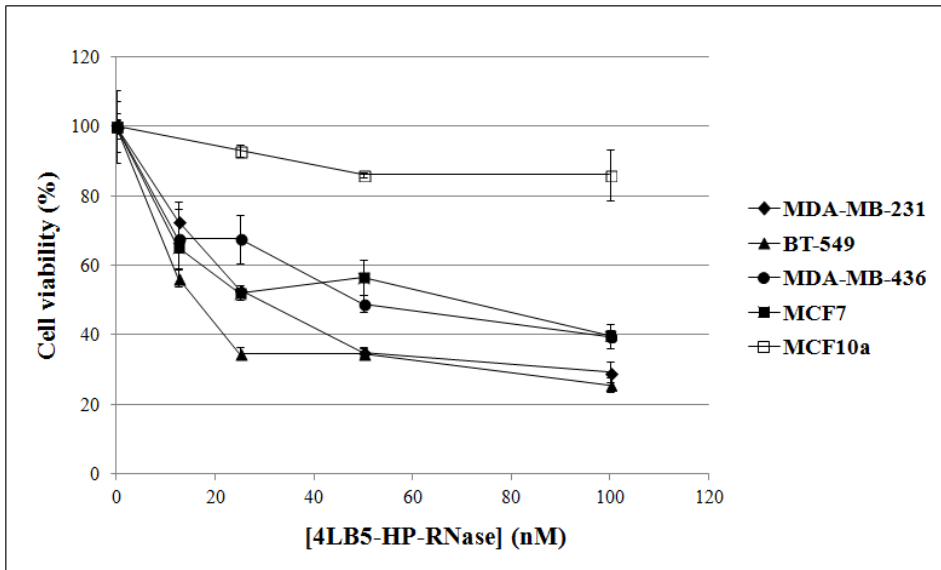


Fig. 16 - *In vitro* effects of the immunoRNase on tumor cell survival. Dose-response curves of NCL-positive MDA-MB-231 (rhomboids), MCF-7 (black squares), BT-549 (triangles) and MDA-MB-436 (circles) breast cancer cells or –negative MCF10a (empty squares) normal-like breast cells treated for 72 h with increasing doses (10-100 nM) of 4LB5-HP-RNase. All the experiments are representative of three independent experiments performed in triplicate. Mean \pm SD is reported

To further confirm the antitumor effects of the new construct, we also tested the effects of 4LB5-HP-RNase on the proliferation of surface-NCL positive MDA-MB-231, MDA-MB-436 and BT-749 breast cancer cells, by colony formation assays. To this aim, the cells were seeded at low density in individual wells of a standard 6-well plate, treated with or without 100 nM of 4LB5-HP-RNase for 72 h and grown for 10 days in normal serum-medium. Colonies were then visualized by crystal violet staining and counted.

The results (Figure 17) indicate that the number of colonies in the sample treated with 4LB5-HP-RNase is much lower than that of negative control cells and significantly reduced with respect to cells treated with the parental 4LB5 scFv, tested in parallel assays, thus indicating that 4LB5-HP-RNase inhibits the proliferation of all treated cells more efficiently than the parental scFv probably due to its acquired RNase activity.

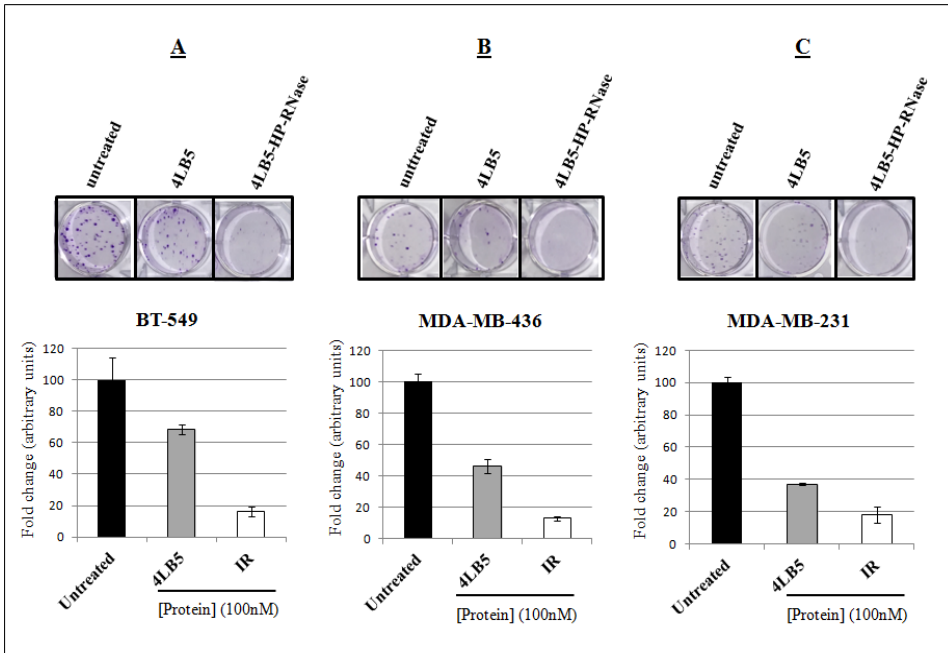


Fig. 17 - *In vitro* effects of 4LB5-HP-RNase on cancer cell proliferation. Colony assays on triple-negative BT-549 (A), MDA-MB-436 (B) and MDA-MB-231 (C) breast cancer cells performed in the absence or in the presence of 100 nM of 4LB5-HP-RNase or 4LB5, tested in parallel assays, and stained after 10 days with Crystal violet. All the experiments are representative of three independent experiments performed in triplicate.

2.5 *4LB5-HP-RNase induces apoptosis in surface NCL-positive cancer cells*

Several recent reports indicate that NCL is a negative regulator of cell apoptosis. The role of cell surface NCL is highlighted by studies showing that functional blockage or down-regulation of cell surface NCL expression inhibits migration and tube formation (84, 85), and causes endothelial-cell apoptosis (86).

To investigate whether the reduction of the viability and proliferation observed for the surface-NCL cells treated with 4LB5-HP-RNase was associated with its ability to induce apoptosis, the MDA-MB-231 triple-negative breast cancer cells were treated with increasing concentrations of 4LB5-HP-RNase (1-200 nM). After 72 hours of

treatments, total cell extracts were analyzed by Western Blotting to measure the reduction of full-length poly(ADP-ribose) polymerase (PARP) levels, which is a pro-apoptotic signal (87).

The results, shown in Figure 18, indicate that 4LB5-HP-RNase induces in treated cells PARP degradation in a dose-dependent manner with the total loss of the PARP-signal following the treatment with 50 nM protein concentration, thus confirming the activation of the apoptotic pathway by the anti-NCL immunRNase.

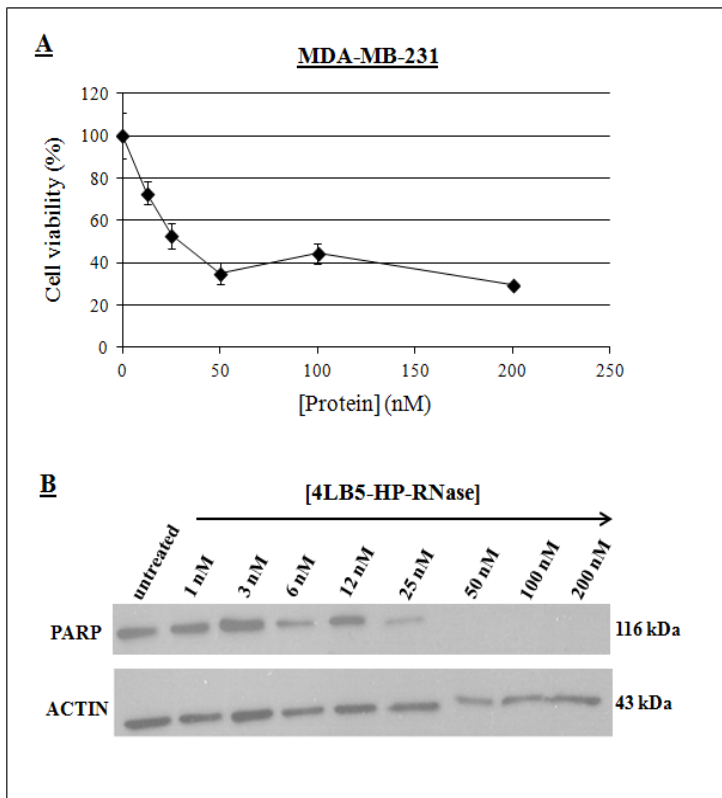


Fig. 18 - Effects of 4LB5-HP-RNase on cancer cell apoptosis. A: Dose-response curve of NCL-positive MDA-MB-231 cells (rhomboids) treated for 72h with increasing doses (10-200 nM) of 4LB5-HP-RNase. **B:** Western Blotting analysis of total lysates from MDA-MB-231 cells treated with increasing concentrations (10-200 nM) of 4LB5-HP-RNase to evaluate inactive-PARP cleavage. Actin was used as loading control.

2.6 Effects of 4LB5-HP-RNase on the levels of oncogenic intracellular and extracellular miRNAs

The importance of NCL in cancer biology was recently highlighted by studies showing that NCL regulates the maturation and the expression of a specific subset of miRNAs, including miR-21, miR-221, miR-222, that are causally involved in breast cancer initiation, progression, and drug resistance (41, 88-91).

In order to assess if the chimeric 4LB5-HP-RNase protein affects the levels of these miRNAs, triple-negative MDA-MB-231 breast cancer cells were treated with increasing doses of 4LB5-HP-RNase and the RNA was extracted after 72 hours of treatment. As shown in Figure 19A, the Real-Time PCR analysis reveals that the levels of the mature forms of miR-21, miR-221 and miR-222 are strongly reduced in a dose-dependent manner by the treatment with 4LB5-HP-RNase with a relevant effect already detectable at the lowest concentration tested for all the miRNAs analyzed.

Previous studies have demonstrated that 4LB5 was already able to inhibit the interaction between NCL and the micro-RNA microprocessor complex impairing the maturation of these NCL-dependent miRNAs (74).

To evaluate if 4LB5-HP-RNase-associated effects on mature miRNAs levels were due also to the effective RNA degradation action of the ribonuclease moiety and not only to the inhibition of the interaction between NCL and microprocessor complex by the scFv domain, MDA-MB-231 cells were treated in parallel assays with equimolar doses of 4LB5 or 4LB5-HP-RNase. As shown in Figure 19B, the immunoRNase impairs the miRNAs levels more efficiently than 4LB5, thus suggesting that the enzymatic activity of the ribonuclease strongly enhances the action of 4LB5 on miRNAs levels.

These results demonstrate that 4LB5-HP-RNase efficiently impairs the levels of miRNAs extensively associated with an invasive phenotype of breast cancer cells resistant to the conventional anti-cancer therapies, and that this effect is due also to its enzymatic activity.

Since cancer cells actively release extracellular vesicles (EVs) into surrounding tissues which play pleiotropic roles in cancer progression, such as immune escape, neovascularization and metastasis, we also tested the effects of 4LB5-HP-RNase on their EV-packed miRNAs. Particularly, oncogenic miR-21, miR-221 and miR-222 were previously demonstrated to be released by colon cancer cells and transferred to other cancer cells, mediating their aggressiveness (92).

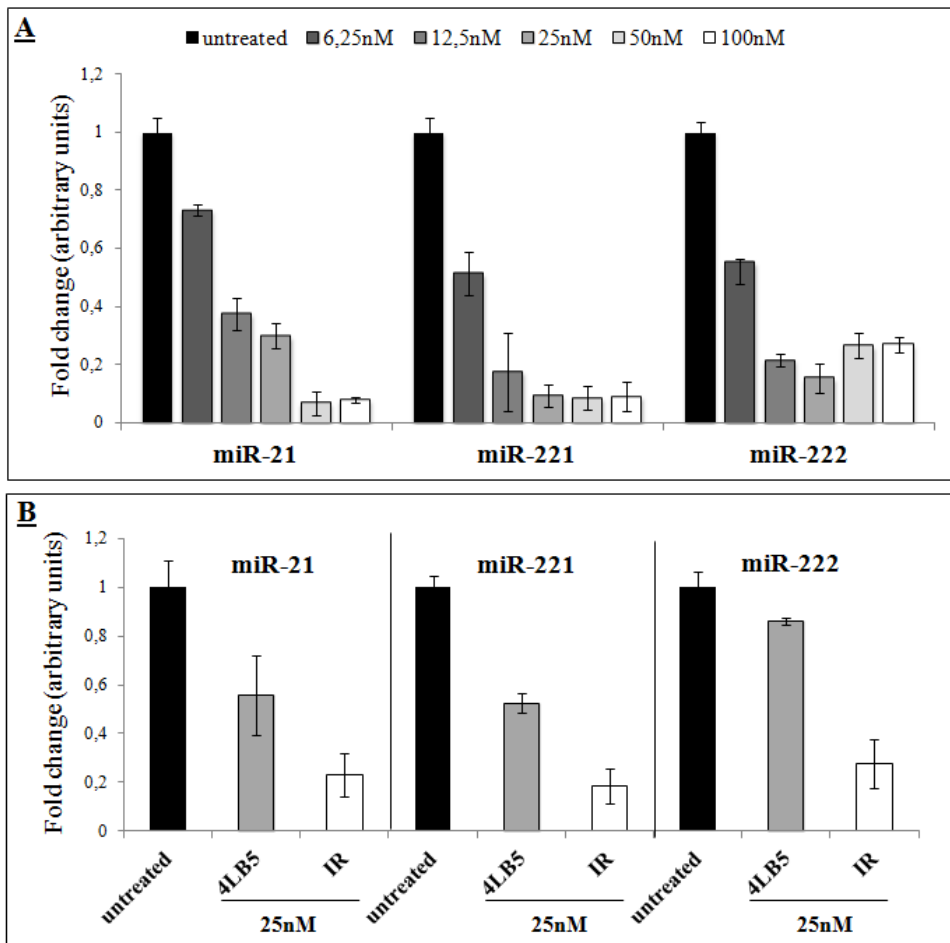


Fig. 19 - Effects of 4LB5-HP-RNase on miRNAs levels in cancer cells. **A:** NCL-dependent mature miR-21, -221 and -222 levels were analyzed by real-time PCR after 72 h of incubation of MDA-MB-231 cells with increasing concentrations (6-100 nM) of 4LB5-HP-RNase. **B:** Comparison between the effects of 4LB5 (grey bars) and 4LB5-HP-RNase (white bars) on mature miR-21, -221 and -222 levels by using an intermediate concentration (25 nM) of chimeric proteins for the treatment of MDA-MB-231 cells. Relative microRNA expression levels were normalized for control untreated sample, and relative abundance (fold change) is reported. Data are the average of three independent experiments performed in triplicate. Mean \pm SD is reported.

In order to investigate the hypothesis that NCL may display a protective role on cancer cell-derived EVs-associated miRNAs, we have tested for the first time the ability of both anti-NCL 4LB5-HP-RNase and 4LB5 scFv to affect the levels of EVs-related miR-21 following the binding and the possible displacement of the Nucleolin from the miR. To this aim we have initially isolated the EVs from the conditioned serum-deprived medium of lymph node metastatic derivatives colorectal SW620 cancer cells which are widely used in literature as model for exosomes studies (93). Then, using a combination of a polymer-based exosome precipitation and a differential centrifugation approach to fractionate the EVs-containing medium, we have isolated the SW620-derived exosomes which were tested for the presence of NCL by western blotting analysis (data not shown). Once confirmed the presence of NCL, EVs were then treated with either 4LB5-HP-RNase or 4LB5 scFv at a concentration of 50 nM for 2 hours at 37°C. The total RNA was extracted and the exosomes-related miR-21 levels were analyzed by Real-Time PCR analysis. RNU48 snoRNA was used as negative control to evaluate the potential contamination of cellular RNAs during the EVs purification procedure.

As shown in Figure 20, 4LB5-HP-RNase strongly reduces the miR-21 levels with respect to the untreated control, whereas the treatment with an equimolar dose of 4LB5, tested in a parallel assay, only slightly affects the miR-21 levels.

These data support the hypothesis that the binding of Nucleolin by the scFv 4LB5 may cause the displacement of the Nucleolin from the miR-21 allowing for the RNase moiety present in 4LB5-HP-RNase to degrade miR-21. Thus, the enzymatic activity of 4LB5-HP-RNase could be responsible for its more potent antitumor effects on extracellular miRNAs, thus indicating a potential role of the anti-NCL immunoRNase in the inhibition of cancer cell-cell communication involved in the tumor progression.

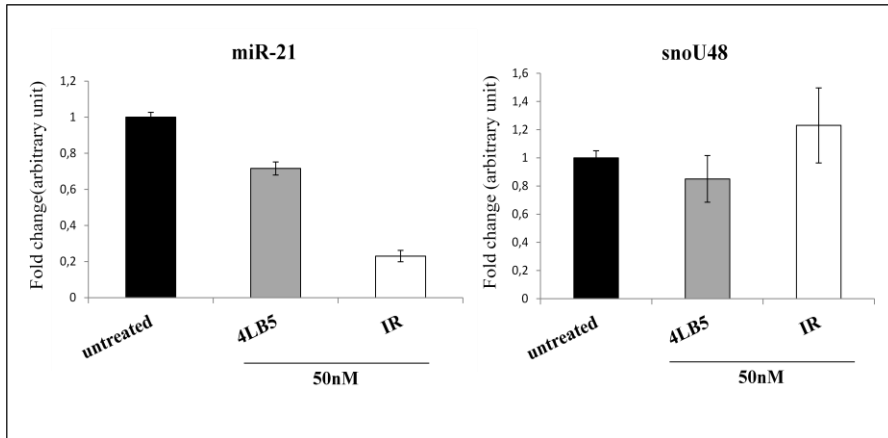


Fig. 20 - Effects of 4LB5-HP-RNase on cancer cells-derived extracellular vesicles-miR-21. The mature miR-21 levels were analyzed by real-time PCR on RNA extracted from exosomes derived from the conditioned medium of SW620 cancer cells treated for 72 h with equimolar doses (50 nM) of 4LB5-HP-RNase (white bars) or 4LB5 (grey bars), tested in a parallel assay. Relative microRNA expression levels were normalized for control untreated sample, and relative abundance (fold change) is reported. The snoRNA RNU48 was used as negative control of RNAs cellular contamination.

2.7 *In vivo* effects of 4LB5-HP-RNase

To evaluate the therapeutic effects of 4LB5-HP-RNase *in vivo*, we generated orthotopic mouse models of human TNBC by injecting surface-NCL positive MDA-MB-231 triple-negative breast cancer cells into the mammary fat pad of Non Obese Diabetic-Severe Combined ImmunoDeficient (NOD-SCID) mice. Two weeks after the injection, groups of five mice bearing tumors of comparable size received intraperitoneal injection of PBS solution or 2 mg/kg 4LB5-HP-RNase, twice weekly. As shown in Figure 21A, four weeks after the first treatment, 4LB5-HP-RNase strongly reduced tumor volume in comparison with those of control mice, thus indicating that it exerts specific antitumor activity *in vivo*.

In order to compare the *in vivo* antitumor effects of 4LB5-HP-RNase with those observed for the parental 4LB5 scFv (74), a second *in vivo* experiment was performed in the same experimental model. Mice bearing tumors of comparable reduced sizes were injected with equimolar doses of 4LB5 or 4LB5-HP-RNase in order to compare their efficacy. As shown in Figure 21B, compared with 4LB5, 4LB5-HP-RNase shows a

stronger antitumor activity even though its larger size could reduce its diffusion into the tumors with respect to the parental scFv. Interestingly, H&E staining (Figure 21C, upper panel) shows reduced cellularity and several areas of necrosis following treatment with the 4LB5-HP-RNase. In addition, Ki-67 staining of treated tumors indicates a reduced proliferation rate compared with controls (Figure 21C, lower panel). During all the treatments, mice did not show signs of wasting, such as loss of weight (Figure 21D) or other visible signs of toxicity, thus suggesting that 4LB5-HP-RNase was not toxic for normal tissues.

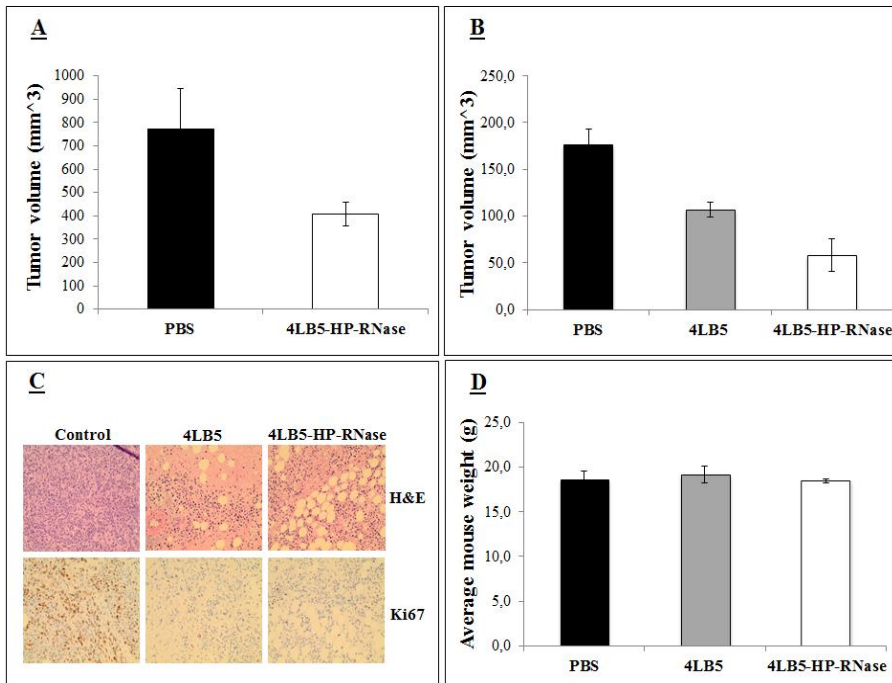


Fig. 21 - A: *In vivo* effects of 4LB5-HP-RNase on NCL-positive tumors induced in mice by using MDA-MB-231 breast cancer cells. **A:** NOD-SCID ($n = 5$) mice were injected with 2×10^6 MDA-MB-231-Luc cells into the mammary fat pad. After 2 weeks, mice were treated with control PBS solution or 2 mg/kg of 4LB5-HP-RNase twice a week. Mice were monitored by IVIS weekly. At 6 weeks from injection (4 weeks of treatment), mice were sacrificed. Tumors were excised and measured. **B:** In a second experiment, mice were treated with equimolar doses of 4LB5 or 4LB5-HP-RNase (2 mg/kg) or with PBS, as described for Figure 21A. **C:** Representative images of H&E and Ki-67 staining of tumors shown in B; 20x magnification is reported. **D:** Weight of mice treated with PBS (black bars), 4LB5 (grey bars) or 4LB5-HP-RNase (white bars).

DISCUSSION

This study aims at the identification of innovative approaches for BC therapies based on the generation and characterization of two immunoRNAses:

1. Breast cancer: novel ErbB2-targeted therapies

ErbB2 amplification is an early event in the development of breast cancer (94, 95) and ErbB2 overexpression is associated with a poor prognosis (6), as the receptor plays a key role in tumor cell growth. Indeed, ErbB2 overexpression on the surface of tumour cells induces the formation of ErbB heterodimers and homodimers, thus leading to an excess of ErbB-mediated signalling, which drives oncogenic cell survival and proliferation (17-19).

Its oncogenic potential, its selective overexpression in human tumors and its accessibility on tumor cell surface make ErbB2 a good target for the development of new anticancer agents, including monoclonal antibodies that target the extracellular domain of the receptor.

The humanized anti-ErbB2 antibody Trastuzumab is widely used for the therapy of breast cancer with some success. However, a high percentage of breast cancer patients are resistant to Trastuzumab treatment and/or manifest adverse side effects, such as cardiac dysfunction (11-15), due to the inhibition in cardiac cells of ErbB2 signalling pathway, which is known to play a key role in survival pathway of cardiomyocytes (16).

Pertuzumab, another humanized anti-ErbB2 antibody recently approved by the FDA for metastatic breast cancer therapy, has shown a limited efficacy in clinical trials. Furthermore, it has been found to induce cardiac dysfunction, although it was not possible to assess whether the rate is similar to that of Trastuzumab. In fact, the limited number of small clinical trials on patients that have already supported Trastuzumab therapy without cardiotoxic effects, provide us with partial and preliminary results (11).

A different approach with respect to ‘naked’ antibodies targeting ErbB2 is the use of antibody–drug conjugates. Recently, Trastuzumab has been conjugated to a maytansine derivative (DM1), a potent antimicrotubule agent, leading to the approval of the new drug, called T-DM1 (8). After the binding to ErbB2, T-DM1 is internalized and DM1 is subsequently released into the cell, thus delivering the chemotherapeutic

agent directly into the cells that overexpress ErbB2 (96). Although T-DM1 has shown encouraging anti-tumor effects in preclinical and early clinical studies (8, 97), it recognizes the same epitope of ErbB2. For this reason, it should have the same limitations of Trastuzumab, such as the same effects on signaling pathways in cardiac cells and a similar inability to recognize resistant cells expressing ErbB2 variant, such as Delta16 (lacking the exon 16) (98), or those cells expressing mucins, such as MUC4 or other receptors, that mask the Trastuzumab epitope (30).

In our laboratory a novel fully human antibody fragment was obtained by phage display: it recognizes an epitope of ErbB2 different from that of Trastuzumab and Pertuzumab and consequently has a different mechanism of action. In particular, it does not show toxic effects on cardiac cells and it is able to inhibit some Trastuzumab resistant tumor cell lines (99).

Furthermore, in order to overcome the limits of toxins, novel fully human immunoconjugates, such as immunoRNases, have been generated in our laboratory by fusing the human anti-ErbB2 scFv, named Erbicin, with human non immunogenic ribonucleases (RNases), that can specifically degrade cellular RNAs and induce tumor cell death once internalized through antibody mediated endocytosis.

In this project of thesis, we have characterized Erb-HP-DDADD-RNase, a fully human inhibitor-resistant immunoRNase targeting the ErbB2 receptor. This immunoRNase was obtained by fusing a variant of human pancreatic RNase (HP-DDADD-RNase), made resistant to RI, with Erbicin, the novel anti-ErbB2 scFv (36, 99).

The novel immunoRNase retains the biological actions of both antibody and RNase moieties. It binds to a panel of ErbB2-positive breast cancer cells expressing different levels of ErbB2 with an affinity comparable to that of the parental scFv, it has an enzymatic activity similar to that of the previously reported immunoRNase Erb-HP-RNase (28), but inhibits the growth of breast cancer cells more efficiently due to its resistance to RI (36).

In this study, we demonstrate that the differential efficacy of the two immunoRNases is highlighted on cell lines expressing low levels of ErbB2 receptor. Indeed, less efficient internalization of the immunoRNases into the cytosol does not affect the cytotoxicity of the novel immunoRNase Erb-HP-DDADD-RNase, but leads to full inhibition of the parental Erb-HP-RNase. In addition, Erb-HP-DDADD-RNase inhibits the growth of Trastuzumab-resistant breast cancer cells *in vitro* and *in vivo* with a greater potency than that of the parental immunoRNase. Finally, in line with the results previously obtained for

the parental immunoRNase (31), Erb-HP-DDADD-RNase does not show cardiotoxic effects either *in vitro* on human cardiomyocytes or *in vivo* on a mouse model (79).

Thus, Erb-HP-DDADD-RNase could be a promising candidate for those patients ineligible for Trastuzumab treatment due to primary or acquired Trastuzumab resistance or due to cardiac dysfunction.

2. A novel approach for triple-negative breast cancer (TNBC) therapy

ErbB2 overexpression has been reported in only 25% of human breast cancers (4), whereas most of them are ErbB2-negative, such as triple negative tumors (TNBC). TNBC is characterized by the absence of estrogen receptor (ER), progesterone receptor (PR) and ErbB2, thus representing a unique subgroup, with a specific molecular profile, lack of effective therapies and aggressive behavior with consequent poor prognosis.

Contrary to other breast cancer subtypes, for which therapies targeting biological drivers of tumorigenesis proved to be successful, no molecular targeted agent is approved for TNBC yet. Thus, it is imperative to develop new strategies able to control TNBC and delay the onset of patient's resistant to chemotherapy.

A new target for immunotherapy of TNBC could be represented by Nucleolin (NCL). NCL is a highly conserved nucleocytoplasmic multifunctional protein, localized in the nucleolus, nucleus and cytoplasm of the cell which participates in many cellular functions under both physiological and pathological conditions. Recent reports show that NCL is frequently up-regulated and selectively expressed on the surface of cancer cells and cancer associated endothelial cells but not on their normal counterparts. Following the interaction with various ligands, surface Nucleolin is implicated directly or indirectly in signal transduction events (70) and plays a critical role in tumorigenesis, tumor invasiveness, inflammation and/or angiogenesis.

NCL is also a major component of the ribosomal RNA nucleolar-processing complex (40, 100) and it is directly involved in miRNA biogenesis (101), including that of miR-10a, miR-21, miR-103, miR-221, and miR-222. Since the miR-21, miR-221 and miR-222 up-regulation has been associated with breast cancer aggressiveness and resistance to antineoplastic therapies (59-62), NCL has a critical protumorigenic function by regulating their biogenesis at the post transcriptional level, thus enhancing their maturation from pri- to pre-miRNAs (41).

Interestingly, miRNAs can also be detected in extracellular compartments (102-105) where they are stably “protected” as they can either be associated with RNA-binding proteins and lipoprotein complexes or they can be packaged into extracellular vesicles (EVs) (105, 106). Furthermore, some studies support a shift of miRNAs from the protein bound to the exosomal compartment (and vice versa) (65), highlighting a novel mechanism of intercellular communication in which RNA-binding proteins, such as NCL, may be associated in complexes for the packaging and export of these miRNAs, thus protecting them from proteases degradation.

Altogether, these data provide evidence that Nucleolin is a promising target for cancer therapy. Indeed, given the continuous and abundant expression in tumor compared to normal cells, tumor cells are the preferential targets of inhibitors of surface Nucleolin without affecting nuclear Nucleolin of normal cells (40). To this aim a number of molecules that target cell surface NCL are being developed as potential anti-cancer therapeutics, such as peptides (HB-19 pseudopeptide or structurally related Nucant pseudopeptides) or aptamers (AS1411). Although promising, they have intrinsic limitations, such as extremely short half-life or undesired immunostimulatory actions that may be a concern if these drugs are used for breast cancer therapy (73).

To overcome these limits, we previously selected by phage-display technology a fully human recombinant anti-NCL scFv, named 4LB5, which specifically binds to NCL on the cell surface of cancer cells. This scFv displayed a significant ability to discriminate between cancer and normal-like breast cells to selectively reduce tumor cell viability, proliferation, and migration, and induce apoptosis in cancer cells. Furthermore, 4LB5 treatment affects the expression of mature miR-21, -221, and -222, by interfering in the NCL interaction with DGCR8 and impairing the maturation of the primary forms of these miRNAs (74).

Based on the ability of 4LB5 to translocate into the cytoplasm following NCL binding, this scFv can be used to vehicle antitumoral molecules directly into cancer cells thus enhancing its therapeutic activity. To this aim, we engineered a novel anti-NCL immunoRNase, named 4LB5-HP-RNase, by fusing the human scFv moiety with the human pancreatic RNase (HP-RNase), thus combining *per se* antitumoral activity of 4LB5 with the enzymatic activity of the ribonuclease, which can be useful to degrade NCL associated miRNAs or intracellular RNAs. Indeed, the novelty of this study has been to combine two activities for selective cancer cell death that, to our knowledge, has never been described for TNBC and appear to be highly promising for its therapy.

Here we describe the construction, characterization and antitumor activity of the novel NCL-targeting immunoRNase. We demonstrate that 4LB5-HP-RNase retains the biological action of both the antibody and RNase moieties. In fact, the novel immunoRNase selectively and efficiently binds to a panel of different surface-NCL positive breast cancer cells but not to normal-like breast cancer, and shows an enzymatic activity comparable to that of the previously characterized IR (Erb-HP-RNase) (28). Moreover, 4LB5-HP-RNase treatment of breast cancer cells, but not of normal-like breast cells, significantly reduces their *in vitro* and *in vivo* growth by inducing apoptosis.

Interestingly, 4LB5-HP-RNase strongly affects the intracellular levels of tumorigenic miR-21, -221, and -222 in breast cancer cells, in a more potent manner with respect to that of 4LB5, thus indicating that the acquired enzymatic activity improves the antitumoral efficacy of 4LB5.

Finally, we report on preliminary critical data suggesting a key role of NCL in EVs-mediated cancer intracellular communication. Here we show that NCL is present in the exosomes released from cancer cells and that the treatment with the anti-NCL IR strongly reduces EVs-associated *miR-21* levels. These data strongly support the hypothesis that NCL may be directly involved in EVs-mediated intracellular communication and that molecules targeting NCL might represent a new important approach to impair it. However, further studies will have to be carried out to investigate the traffic of both NCL and miRNAs in EVs and their molecular association.

In summary, here we describe a new approach for immunotherapy of TNBC based on a novel fully human NCL-targeting immunoconjugate with potent antineoplastic activity that could be useful for the treatment of different types of carcinoma, ineligible to Trastuzumab treatment or to other currently available targeted therapies.

REFERENCES

1. Ferlay J, Soerjomataram I, Dikshit R et al. "Cancer incidence and mortality worldwide: sources, methods and major patterns in GLOBOCAN 2012". *Int J Cancer*, 136(5):E359-86 (2015).
2. Erika V. et al. "Trial Watch: Tumor-targeting monoclonal antibodies in cancer therapy". *Oncoimmunology*, 3:e27048 (2014).
3. Fukushige S. et al. "Localization of a novel v-erbB-related gene, c-erbB-2, on human chromosome 17 and its amplification in a gastric cancer cell line". *Mol Cell Biol*, 6(3):955-8 (1986).
4. Slamon D.J. et al. "Studies of the HER-2/neu proto-oncogene in human breast and ovarian cancer". *Science*, 244(4905):707-12 (1989).
5. Tagliabue E. et al. "Selection of monoclonal antibodies which induce internalization and phosphorylation of p185HER2 and growth inhibition of cells with HER2/NEU gene amplification". *Int J Cancer*, 47(6):933-7 (1991).
6. Albanell J., Baselga J. "Mechanism of action of anti-HER2 monoclonal antibodies". *Ann Oncol*, 12 Suppl 1:S35-41 (2001).
7. Sabatier R., Gonçalves A. "Pertuzumab (Perjeta®) approval in HER2-positive metastatic breast cancers". *Bull Cancer*, 101(7-8):765-71 (2014).
8. Lewis Phillips et al. "Targeting HER2-positive breast cancer with trastuzumab-DM1, an antibody-cytotoxic drug conjugate". *Cancer Res*. 68, 9280-9290 (2008).
9. Stebbing J. et al. "Herceptin (trastuzumab) in advanced breast cancer". *Cancer Treat Rev*, 26(4):287-90 (2000).
10. Romond E.H. et al. "Trastuzumab plus adjuvant chemotherapy for operable HER2-positive breast cancer". *N Engl J Med*, 353(16):1673-84 (2005).
11. Lenihan D. et al. "Pooled analysis of cardiac safety in patients with cancer treated with pertuzumab". *J Ann Oncol*, 23(3):791-800 (2012).
12. Sendur M.A. et al. "Cardiotoxicity of novel HER2-targeted therapies". *Curr Med Res Opin*, 29(8):1015-24 (2013).
13. Slamon D.J. et al. "Use of chemotherapy plus a monoclonal antibody against HER2 for metastatic breast cancer that overexpresses HER2". *N Engl J Med*, 344(11):783-92 (2001).
14. Nahta R. et al. "Mechanisms of disease: understanding resistance to HER2-targeted therapy in human breast cancer". *Nat Clin Pract Oncol.*, 3(5):269-80 (2006).
15. Seidman A. et al. "Cardiac dysfunction in the trastuzumab clinical trials experience". *J Clin Oncol.*, 20(5):1215-21 (2002).
16. Fedele C. et al. "Mechanisms of cardiotoxicity associated with ErbB2 inhibitors". *Breast Cancer Res Treat*, 134(2):595-602 (2012).
17. Klapper L.N. et al. "Biochemical and clinical implications of the ErbB/HER signaling network of growth factor receptors". *Adv Cancer Res*, 77:25-79 (2000).
18. Busse D. et al. "HER-2/neu (erbB-2) and the cell cycle". *Semin Oncol*, 27(6 Suppl 11):3-8; discussion 92-100 (2000).
19. Baselga J., Swain S.M. "Novel anticancer targets: revisiting ERBB2 and discovering ERBB3". *Nat Rev Cancer.*, 9(7):463-75 (2009).
20. Griffiths A.D. et al. "Isolation of high affinity human antibodies directly from large synthetic repertoires". *EMBO J*, 13(14):3245-60 (1994).
21. Pastan I., FitzGerald D. "Recombinant toxins for cancer treatment". *Science*, 254(5035):1173-7 (1991).

22. Carter P. "Improving the efficacy of antibody-based cancer therapies". *Nat Rev Cancer*, 1(2):118-29 (2001).
23. Zhang Q. et al. "Monoclonal antibodies as therapeutic agents in oncology and antibody gene therapy". *Cell Res*, 17(2):89-99 (2007).
24. Reiter Y., Pastan I. "Recombinant Fv immunotoxins and Fv fragments as novel agents for cancer therapy and diagnosis". *Trends Biotechnol*, 16(12):513-20 (1998).
25. Gould B.J. et al. "Phase I study of an anti-breast cancer immunotoxin by continuous infusion: report of a targeted toxic effect not predicted by animal studies". *J Natl Cancer Inst*, 81(10):775-81 (1989).
26. Schindler J. et al. "The toxicity of deglycosylated ricin A chain-containing immunotoxins in patients with non-Hodgkin's lymphoma is exacerbated by prior radiotherapy: a retrospective analysis of patients in five clinical trials". *Clin Cancer Res*, 7(2):255-8 (2001).
27. De Lorenzo C. et al. "A new human antitumor immunoreagent specific for ErbB2". *Clin Cancer Res*, 8(6):1710-9 (2002).
28. De Lorenzo C. et al. "A fully human antitumor immunorNase selective for ErbB-2-positive carcinomas". *Cancer Res*, 64(14):4870-4 (2004).
29. De Lorenzo C., D'Alessio G. "Human anti-ErbB2 immunoagents--immunorNases and compact antibodies". *FEBS J*, 276(6):1527-35 (2009).
30. Gelardi T. et al. "Two novel human anti-ErbB2 immunoagents are active on trastuzumab-resistant tumours". *Br J Cancer*, 102(3):513-9 (2010).
31. Riccio G. et al. "Cardiotoxic effects, or lack thereof, of anti-ErbB2 immunoagents". *FASEB J*, 23(9):3171-8 (2009).
32. Fedele C. et al. "Comparison of preclinical cardiotoxic effects of different ErbB2 inhibitors". *Breast Cancer Res Treat*, 133(2):511-21 (2012).
33. Haigis M.C. et al. "Ribonuclease inhibitor as an intracellular sentry". *Nucleic Acids Res*, 31(3):1024-32 (2003).
34. Dickson K.A. et al. "Ribonuclease inhibitor: structure and function". *Prog Nucleic Acid Res Mol Biol*, 80:349-74 (2005).
35. Johnson R.J., et al. "Inhibition of human pancreatic ribonuclease by the human ribonuclease inhibitor protein". *J Mol Biol*, 368(2):434-49 (2007).
36. Riccio G. et al. "A novel fully human antitumor immunorNase resistant to the RNase inhibitor". *Protein Eng Des Sel*, (3):243-8 (2013).
37. Lehmann B.D. et al. "Identification of human triple-negative breast cancer subtypes and preclinical models for selection of targeted therapies". *J Clin Invest*, 121(7):2750-67 (2011).
38. Senkus E. et al. "Time for more optimism in metastatic breast cancer?". *Cancer Treat Rev.*, 40(2):220-8 (2014).
39. Bugler B. et al. "Detection and localization of a class of proteins immunologically related to a 100-kDa nucleolar protein". *Eur J Biochem*, 128(2-3):475-480 (1982).
40. Srivastava M., Pollard H.B. "Molecular dissection of Nucleolin's role in growth and cell proliferation: new insights". *FASEB J.*, 13(14):1911-22 (1999).
41. Pichiorri F. et al. "In vivo NCL targeting affects breast cancer aggressiveness through miRNA regulation". *J Exp Med.*, 210(5):951-68 (2013).
42. Borer R.A. et al. "Major nucleolar proteins shuttle between nucleus and cytoplasm". *Cell*, 56(3):379-390 (1989).
43. Mongelard F., Bouvet P. "Nucleolin: A multiFACeTed protein". *Trends Cell Biol*, 17(2):80-86 (2007).

44. Mi Y. et al. "Apoptosis in leukemia cells is accompanied by alterations in the levels and localization of Nucleolin". *J Biol Chem*, 278(10): 8572-9 (2003).
45. Krust B. et al. "The anti-HIV pentameric pseudopeptide HB-19 is preferentially taken up in vivo by lymphoid norgans where it forms a complex with Nucleolin". *Proc Natl Acad Sci U S A*; 98(24): 14090-5 (2001).
46. Shi H. et al. "Nucleolin is a receptor that mediates antiangiogenic and antitumor activity of endostatin". *Blood*, 110(8): 2899-906 (2007).
47. Tate A. et al. "Met-Independent Hepatocyte Growth Factor-mediated regulation of cell adhesion in human prostate cancer cells". *BMC Cancer*, 6: 197 (2006).
48. Turck N. et al. "Effect of laminin-1 on intestinal cell differentiation involves inhibition of nuclear Nucleolin". *J Cell Physiol*, 206(2): 545-55 (2006).
49. Qiu W. et al. "Overexpression of Nucleolin and different expression sites both related to the prognosis of gastric cancer". *APMIS*, (2013).
50. Legrand D. et al. "Surface Nucleolin participates in both the binding and endocytosis of lactoferrin in target cells". *Eur J Biochem*, 271(2): 303-17 (2004).
51. Christian S. et al. "Nucleolin expressed at the cell surface is a marker of endothelial cells in angiogenic blood vessels". *J Cell Biol*, 163(4): 871-8 (2003).
52. Semenkovich C.F. et al. "A protein partially expressed on the surface of HepG2 cells that binds lipoproteins specifically is Nucleolin". *Biochemistry*; 29(41): 9708-13 (1990).
53. Krust B. et al. "Suppression of tumorigenicity of rhabdoid tumor derived G401 cells by the multivalent HB-19 pseudopeptide that targets surface Nucleolin". *Biochimie*; 93(3): 426-33 (2011).
54. Jordan P. et al. "Major cell surface-located protein substrates of an ecto-protein kinase are homologs of known nuclear proteins". *Biochemistry*; 33(49): 14696-706 (1994).
55. Reyes-Reyes E.M., Akiyama S.K. "Cell-surface Nucleolin is a signal transducing P selectin binding protein for human colon carcinoma cells". *Exp Cell Res*; 314(11-12): 2212-23 (2008).
56. Hoja-Lukowicz D. et al. "The new face of Nucleolin in human melanoma". *Cancer Immunol Immunother*; 58(9): 1471-80. 39 (2009).
57. Galzio R. et al. "Glycosilated Nucleolin as marker for human gliomas". *J Cell Biochem*; 113(2): 571-9 (2012).
58. Koutsoumpa M. et al. "Interplay between alphavbeta3 integrin and Nucleolin regulates human endothelial and glioma cell migration". *J Biol Chem*; 288(1): 343-54 (2013).
59. Di Leva G. et al. "MicroRNA cluster 221-222 and estrogen receptor alpha interactions in breast cancer". *J Natl Cancer Inst*, 102(10):706-21 (2010).
60. Iliopoulos D. et al. "STAT3 activation of miR-21 and miR-181b-1 via PTEN and CYLD are part of the epigenetic switch linking inflammation to cancer". *Mol Cell*, 39(4):493-506 (2010).
61. Martello G. et al. "A MicroRNA targeting dicer for metastasis control". *Cell*, 141(7):1195-207 (2010).
62. Farazi T.A. et al. "MicroRNA sequence and expression analysis in breast tumors by deep sequencing". *Cancer Res*, 71(13):4443-53 (2011).
63. Wang K. et al. "Export of microRNAs and microRNA-protective protein by mammalian cells". *Nucleic Acids Res*, 38(20):7248-59 (2010).
64. They C. et al. "Membrane vesicles as conveyors of immune responses". *Nat Rev Immunol*, 9: 581_93 (2009).

65. Valadi H. et al. "Exosome-mediated transfer of mRNAs and microRNAs is a novel mechanism of genetic exchange between cells". *Nat Cell Biol.*, 9:654_9 (2007).
66. Gyorgy B. et al. "Membrane vesicles, current state-of-the-art: emerging role of extracellular vesicles". *Cell Mol Life Sci.*, 68: 2667_88.5 (2011).
67. Choi D.S. et al. "The protein interaction network of extracellular vesicles derived from human colorectal cancer cells". *J Proteome Res.*, 11:1144_51 (2012).
68. Hovanesian A.G. et al. "Surface expressed Nucleolin is constantly induced in tumor cells to mediate calciumdependent ligand internalization". *PLoS One*, 5(12): e15787 (2010).
69. Bates P.J. et al. "Discovery and development of the G-rich oligonucleotide AS1411 as a novel treatment for cancer". *Exp Mol Pathol*, 86(3):151–164 (2009).
70. Koutsioumpa M., Papadimitriou E. "Cell surface Nucleolin as a target for anticancer therapies". *Recent Pat Anticancer Drug Discov*, 9(2):137–152 (2014).
71. Destouches D. et al. "Suppression of tumor growth and angiogenesis by a specific antagonist of the cell-surface expressed Nucleolin". *PLoS ONE*, 3(6):e2518 (2008).
72. El Khoury D. et al. "Targeting surface Nucleolin with a multivalent pseudopeptide delays development of spontaneous melanoma in RET transgenic mice". *BMC Cancer*, 10:325 (2010).
73. Abdelmohsen K., Gorospe M. "RNA-binding protein Nucleolin in disease". *RNA Biol*, 9(6):799–808 (2012).
74. Palmieri D. et al. "Human anti-Nucleolin recombinant immunoagent for cancer therapy". *Proc Natl Acad Sci U S A*, 112(30):9418-23 (2015).
75. Sambrook J. et al. "Molecular Cloning: a Laboratory Manual". Second Edition, Cold Spring Harbor Laboratory Press, Cold Spring Harbor, New York, 9.16 (1989).
76. Laemmli U.K. "Cleavage of structural proteins during the assembly of the head of bacteriophage T4". *Nature*, 227(5259):680-5 (1970).
77. Bartholeyns J. et al. "Explanation of the observation of pancreatic ribonuclease activity at pH 4.5". *Int J Pept Protein Res.*, 10(2):172-5 (1977).
78. Borriello M. et al. "A novel fully human antitumour immunoRNase targeting ErbB2-positive tumours". *Br J Cancer*, 104(11):1716-23 (2011).
79. D'Avino C. et al. "Effects of a second-generation human anti-ErbB2 ImmunoRNase on trastuzumab-resistant tumors and cardiac cells". *Protein Eng Des Sel.*, 27(3):83-8 (2014).
80. De Lorenzo C. et al. "Intracellular route and mechanism of action of ERB-hRNase, a human anti-ErbB2 anticancer immunoagent". *FEBS Lett.*, 581(2):296-300 (2007).
81. Ugrinova I. et al. "Inactivation of Nucleolin leads to nucleolar disruption, cell cycle arrest and defects in centrosome duplication". *BMC Mol Biol*, 8: 66 (2007).
82. Ma N. et al. "Nucleolin functions in nucleolus formation and chromosome congression". *J Cell Sci*, 120(Pt 12): 2091-105 (2007).
83. Xu Z. et al. "Knocking down Nucleolin expression in gliomas inhibits tumor growth and induces cell cycle arrest". *J Neurooncol*, 108(1): 59-67 (2012).
84. Huang Y. et al. "The angiogenic function of Nucleolin is mediated by vascular endothelial growth factor and nonmuscle myosin". *Blood*, 107(9): 3564-71 (2006).
85. Koutsioumpa M. et al. "Pleiotrophin expression and role in physiological angiogenesis in vivo: Potential involvement of Nucleolin". *Vasc Cell*, 4: 4 (2012).
86. Fogal V. et al. "Cell surface Nucleolin antagonist causes endothelial cell apoptosis and normalization of tumor vasculature". *Angiogenesis*, 12(1): 91- 100 (2009).
87. Fan T.J. et al. "Caspase family proteases and apoptosis". *Acta Biochim Biophys Sin (Shanghai)*, 37(11):719-27 (2005).

88. Rao X. et al. "MicroRNA-221/222 confers breast cancer fulvestrant resistance by regulating multiple signaling pathways". *Oncogene*, 30(9):1082–1097 (2011).
89. Pogribny I.P. et al. "Alterations of microRNAs and their targets are associated with acquired resistance of MCF-7 breast cancer cells to cisplatin". *Int J Cancer*, 127(8): 1785–1794 (2010).
90. Anastasov N. et al. "Radiation resistance due to high expression of miR-21 and G2/M checkpoint arrest in breast cancer cells". *Radiat Oncol*, 7:206 (2012).
91. Mei M. et al. "Downregulation of miR-21 enhances chemotherapeutic effect of taxol in breast carcinoma cells". *Technol Cancer Res Treat*, 9(1):77–86 (2010).
92. Mitsuru Chiba et al. "Exosomes secreted from human colorectal cancer cell lines contain mRNAs, microRNAs and natural antisense RNAs, that can transfer into the human hepatoma HepG2 and lung cancer A549 cell lines". *Oncol Rep.*, 28(5): 1551–1558 (2012).
93. Dong-Sic Choi et al. "Quantitative proteomics of extracellular vesicles derived from human primary and metastatic colorectal cancer cells." *J Extracell Vesicles*, doi: 10.3402/jev.v1i0.18704. eCollection (2012).
94. Liu E. et al. "The HER2 (c-erbB-2) oncogene is frequently amplified in in situ carcinomas of the breast". *Oncogene*, 7, 1027–1032 (1992).
95. Park K. et al. "HER2 status in pure ductal carcinoma in situ and in the intraductal and invasive components of invasive ductal carcinoma determined by fluorescence in situ hybridization and immunohistochemistry". *Histopathology*, 8, 702–707 (2006).
96. Verma S. et al. "EMILIA Study Group Trastuzumab emtansine for HER2-positive advanced breast cancer". *N Engl J Med.*, 367(19):1783-91 (2012).
97. Burris H.A. 3rd et al. "Phase II study of the antibody drug conjugate trastuzumab-DM1 for the treatment of human epidermal growth factor receptor 2 (HER2)-positive breast cancer after prior HER2-directed therapy". *J Clin Oncol.*, 29(4):398-405 (2011).
98. Marchini C. et al. "The human splice variant Δ 16HER2 induces rapid tumor onset in a reporter transgenic mouse". *PLoS One*, 6(4):e18727 (2011).
99. Troise F. et al. "A novel ErbB2 epitope targeted by human antitumor immunoagents". *FEBS J.*, 278(7):1156-66 (2011).
100. Ginisty H. et al. "Nucleolin functions in the first step of ribosomal RNA processing". *EMBO J.*, 17(5):1476-86 (1998).
101. Pickering B.F. et al. "Nucleolin protein interacts with microprocessor complex to affect biogenesis of microRNAs 15a and 16". *J Biol Chem.*, 286(51):44095-103 (2011).
102. Mitchell P.S. et al. "Circulating microRNAs as stable bloodbased markers for cancer detection". *Proc Natl Acad Sci U S A*, 105:10513–8 (2008).
103. Lawrie C.H. et al. "Detection of elevated levels of tumourassociated microRNAs in serum of patients with diffuse large B-cell lymphoma". *Br J Haematol*, 141:672–5 (2008).
104. Chen X. et al. "Characterization of microRNAs in serum: a novel class of biomarkers for diagnosis of cancer and other diseases". *Cell Res*; 18:997–1006 (2008).
105. Creemers E.E. et al. "Circulating microRNAs: novel biomarkers and extracellular communicators in cardiovascular disease?" *Circ Res*; 110:483–95 (2012).
106. Cortez M.A. et al. "MicroRNAs in body fluids--the mix of hormones and biomarkers". *Nat Rev Clin Oncol*; 8:467–77 (2011).